UC 11, 62

ENVIRONMENTAL EFFECTS OF SOLAR THERMAL POWER SYSTEMS

ENVIRONMENTAL CONSIDERATIONS IN SITING A SOLAR-COAL HYBRID POWER PLANT

II AIR QUALITY AND METEOROLOGICAL IMPACTS

FEBRUARY 1981

PREPARED FOR

U.S. DEPARTMENT OF ENERGY

Contract No. DE-AM03-76-SF00012

LABORATORY OF BIOMEDICAL AND ENVIRONMENTAL SCIENCES
UNIVERSITY OF CALIFORNIA, LOS ANGELES

NOTICE

Printed in the United States of America
Available from
National Technical Information Service
U.S. Department of Commerce
5285 Port Royal Road
Springfield, VA 22161

NTIS price codes
Printed copy:$ 9.00
Microfiche copy:$ 3.50

UCLA 12-1283
UC 11, 62

ENVIRONMENTAL CONSIDERATIONS IN SITING A SOLAR-COAL HYBRID POWER PLANT

II Air Quality and Meteorological Impacts

Donald B. Hunsaker, Jr.
Carolyn T. Hunsaker
Richard L. Perrine

Environmental Science and Engineering
University of California, Los Angeles
November 1980

Prepared for

U.S. DEPARTMENT OF ENERGY

Contract No. DE-AM03-76-SF00012
between the U.S. DOE and the University of California

Laboratory of Biomedical and Environmental Sciences
University of Callifornia, Los Angeles
900 Veteran Avenue
Los Angeles, California 90024

ACKNOWLEDGMENTS

This report topic was used as a theme for multidisciplinary course work offered by the UCLA interdepartmental graduate program in Environmental Science and Engineering. We wish to acknowledge the contributions of the following faculty and graduate students preparing for the D.Env. degree.

Graduate Students

Harlan Hashimoto - M.S. Environmental Health Science, University of Hawaii

Carolyn Hunsaker - M.A. Biology, Loma Linda University

Donald Hunsaker - M.S. Chemistry, Wayne State University

Michael Simpson - M.S. Energy and Resources, University of California, Berkeley

ESE Faculty Advisors and Editors

Dr. Robert G. Lindberg

Dr. Richard L. Perrine

We also wish to acknowledge the help received from Dr. Alan Z. Ullman, Energy Systems Group, Rockwell International in interpreting the system concept studied and review of the report.

ABSTRACT

A study to identify environmental constraints to siting a conceptual solar/coal hybrid power plant revealed that air quality and meteorological considerations, both off-site and on-site were likely to impact both land-use requirements and plant operations (Vol. I). This volume presents a more detailed treatment of these concerns including assumptions and methods of analysis.

It was found that the hybrid plant was not likely to significantly effect either local or regional climate. Microclimatological effects would probably occur within and near the facility but the effects were not quantified. For worst-case scenarios, as much as several hundred grams of particulate matter from coal combustion might deposit on a single heliostat in a 30-day period. Salt particles deposited from cooling tower operation and off-site fugitive dust sources (including crop dusting) could add comparable amounts under their respective worst-case scenarios. Natural and fugitive emissions from coal handling could also deposit significant but unquantified amounts of matter. Thus, a worst-case estimate would be that as much as kilogram quantities of matter could be deposited per heliostat in a 30-day period. The implications of these findings are presented along with recommendations for studies to resolve the uncertainties inherent in the assumptions made for the purposes of this study.

TABLE OF CONTENTS

TABLE OF CONTENTS, (Continued)

LIST OF TABLES

LIST OF TABLES, (Continued)

LIST OF FIGURES

LIST OF FIGURES, (Continued)

ENVIRONMENTAL ASSESSMENT OF A 430 MWe COAL/SOLAR HYBRID POWER PLANT

Volume II. Air Quality and Meteorology Impacts

1.0 INTRODUCTION

The purpose of this study is to identify constraints to siting a coal/solar hybrid power plant. The study is preliminary in nature because many details for such a conceptual facility are uncertain. Thus the study has focused on identifying key constraints that should be studied further in order to facilitate the construction and operation of a coal/solar hybrid plant. Volume I addresses all of the constraints identified through the study. Because primary concern developed around air quality and meteorological impacts, it was decided to incorporate this more lengthy and detailed treatment of the concern in the present separate volume.

Impact assessment requires the collection of environmental data which, to be useful, often must be site-specific. In order to minimize the share of effort devoted to data gathering and focus on potential constraints, a site was selected suited to the conceptual facility but also for which a detailed environmental assessment had already been published. The site for the once proposed Sundesert nuclear plant, in eastern Riverside County, California, near the town of Palo Verde, California, was chosen for this study because it met both criteria. Additional information on the site is presented in Volume I.

The rationale behind this study is that identifying potentially significant impacts at an early stage in the development of the hybrid plant will allow future efforts to focus on in-depth impact assessments of key issues. Thus, in the language of the California Environmental Quality Act, this study serves as an initial study on which a focused environmental impact report can be based.

This study, and particularly, the present Volume II, is somewhat different from a traditional environmental assessment that examines the impacts of a project on the environment. Volume II focuses on intra-plant impacts, i.e., the impacts of one plant subsystem on another, and the impacts of the environment on the plant. The following issues, which are discussed in the present Volume, were selected for analysis because at the outset of this study they were considered to be potentially significant:

- the impact of the deposition of particles from coal combustion on heliostat surfaces,
- the impact of the deposition of salt particles from cooling tower operation on heliostat surfaces;

- the impact of the coal plume on the solar subsystem through attenuation of insolation;

- the impact of the deposition of fugitive and natural particle emissions on heliostat surfaces;

- the impact of the plant on its surroundings via the atmosphere.

Because of limited resources and data gaps, none of these impacts were satisfactorily quantified, in accordance with desired goals for a study such as this. Also, additional potentially significant impacts may exist which have not been covered within this study; consequently, recommendations for future work are found throughout this volume.

This report is organized in the following manner. Chapter 1.0 presents an overview of this study--its purpose, rationale and scope. Chapter 2.0 presents a brief discussion of the technology proposed for utilization. Chapters 3.0 through 7.0 discuss the five issues listed above, respectively. Chapter 8.0 presents conclusions and recommendations for future work.

2.0 SYSTEM DESCRIPTION

The particular coal/solar hybrid plant design upon which this study is based was developed by the Energy Systems Group of Rockwell International Corporation, with assistance from other groups (2.1). The purpose of the Solar Central Receiver Coal Hybrid Power System is to provide a reliable and consistent supply of electricity in a manner that reduces consumption of non-renewable energy resources. The coal/solar hybrid plant consists of three major subsystems: solar collector, coal burner and thermal storage. The plant is essentially a 430 MWe solar power plant with coal combustion and thermal storage back-up systems. If at anytime the solar subsystem cannot generate sufficient electricity to meet demand, then either the thermal storage or coal combustion subsystems are activated to meet demand. Figure 2-1 presents an artist's conception of the plant, Figure 2-2 presents a map view of the plant and its dimensions, and Figure 2-3 illustrates the power flow in the plant.

The solar subsystem consists of a field of 61,000 heliostats which focus insolation on the top of a central tower. Liquid sodium is heated within the tower by this concentration of solar energy. The coal subsystem consists of a coal-fired heater that also heats liquid sodium. The storage subystem is made up of large tanks that hold the hot liquid sodium produced by either solar energy collection or coal combustion. Liquid sodium is thus the working fluid for the system--it is heated, and this heat is used to turn water into steam, which in turn is used to drive a steam turbine generator, thereby producing 430 MWe of electricity at maximum output.

Chapter 2.0 of Volume I of this study presents a detailed description of the system technology; for an even more-detailed description, the reader is referred to reference 2.1.

2.1 References

2.1 Rockwell International, University of Houston, McDonnell Douglas, Salt River Project, Stearns-Roger, Babcock and Wilcox, and SRI International, "Solar Central Receiver Hybrid Power Systems, Sodium-Cooled Receiver Concept." Final Report, Books 1 and 2, Prepared for the U.S. Department of Energy as part of Contract No. DE-AC03-78ET20567 (ET-78-C-03-2233), January 1980.

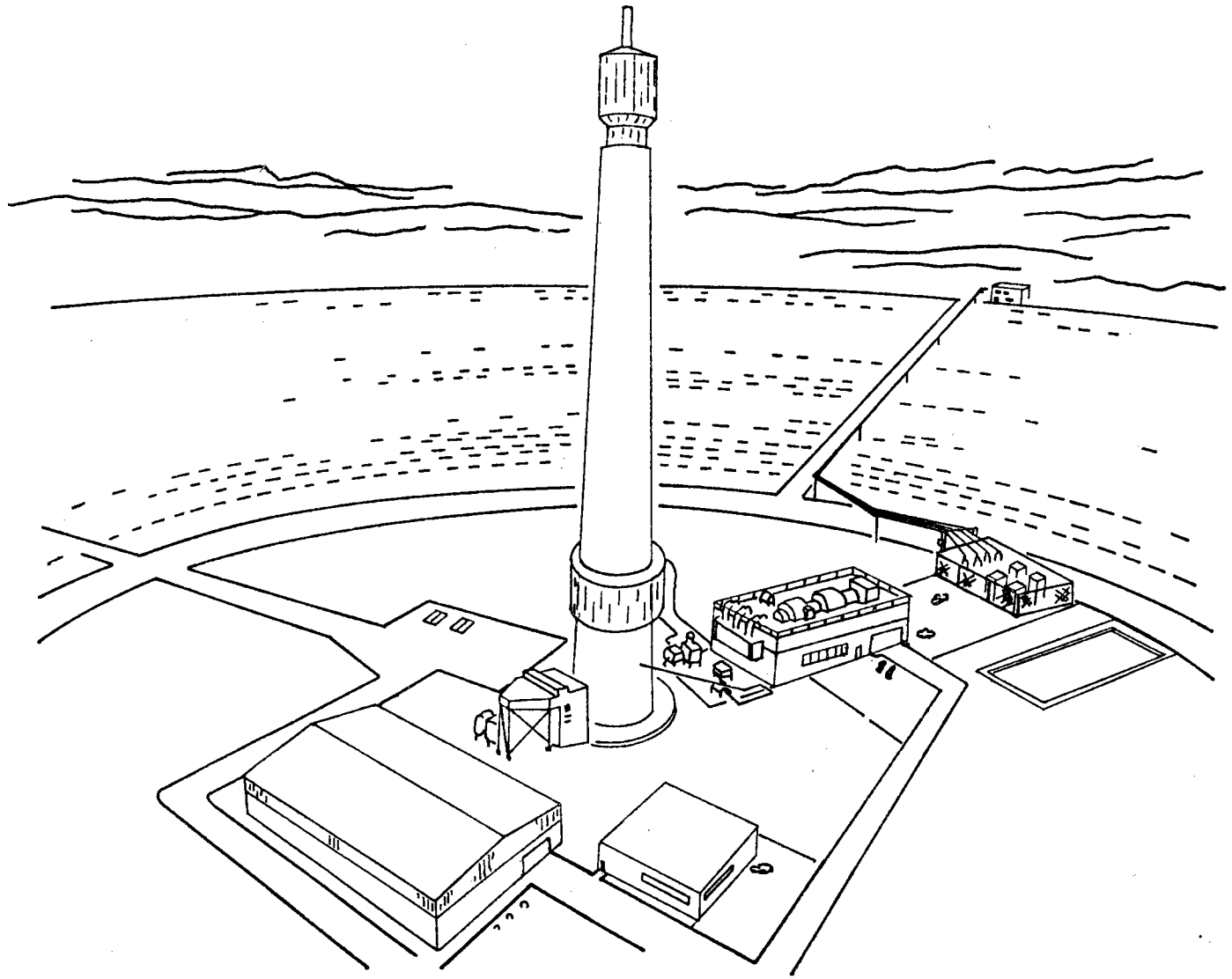

Figure 2-1 Solar Central Receiver Hybrid Power System (1.2)

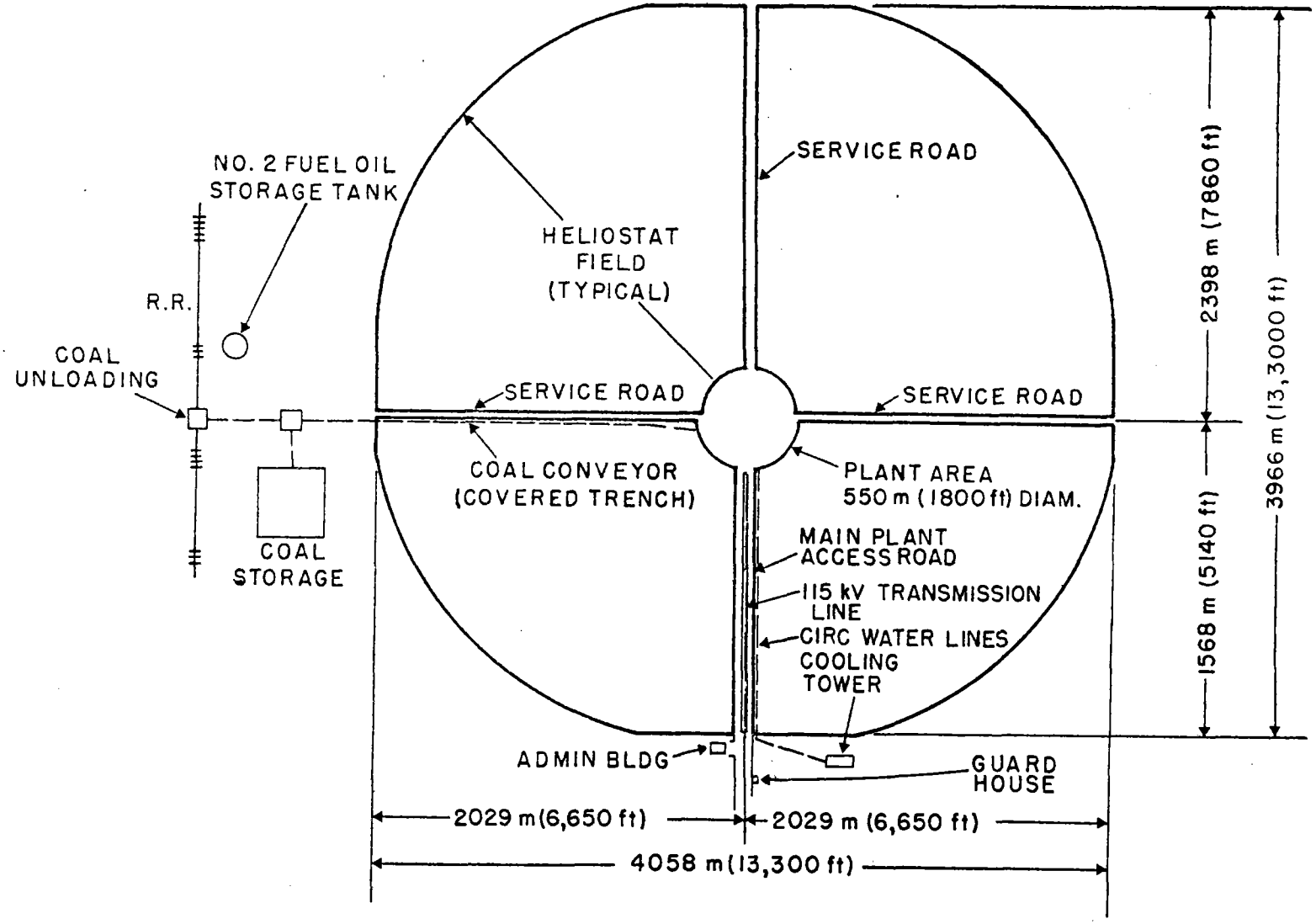

Figure 2-2 Preliminary Plot Plan for 430 MW(e), 1.44 Solar Multiple Commercial Plant
Reference 2.5

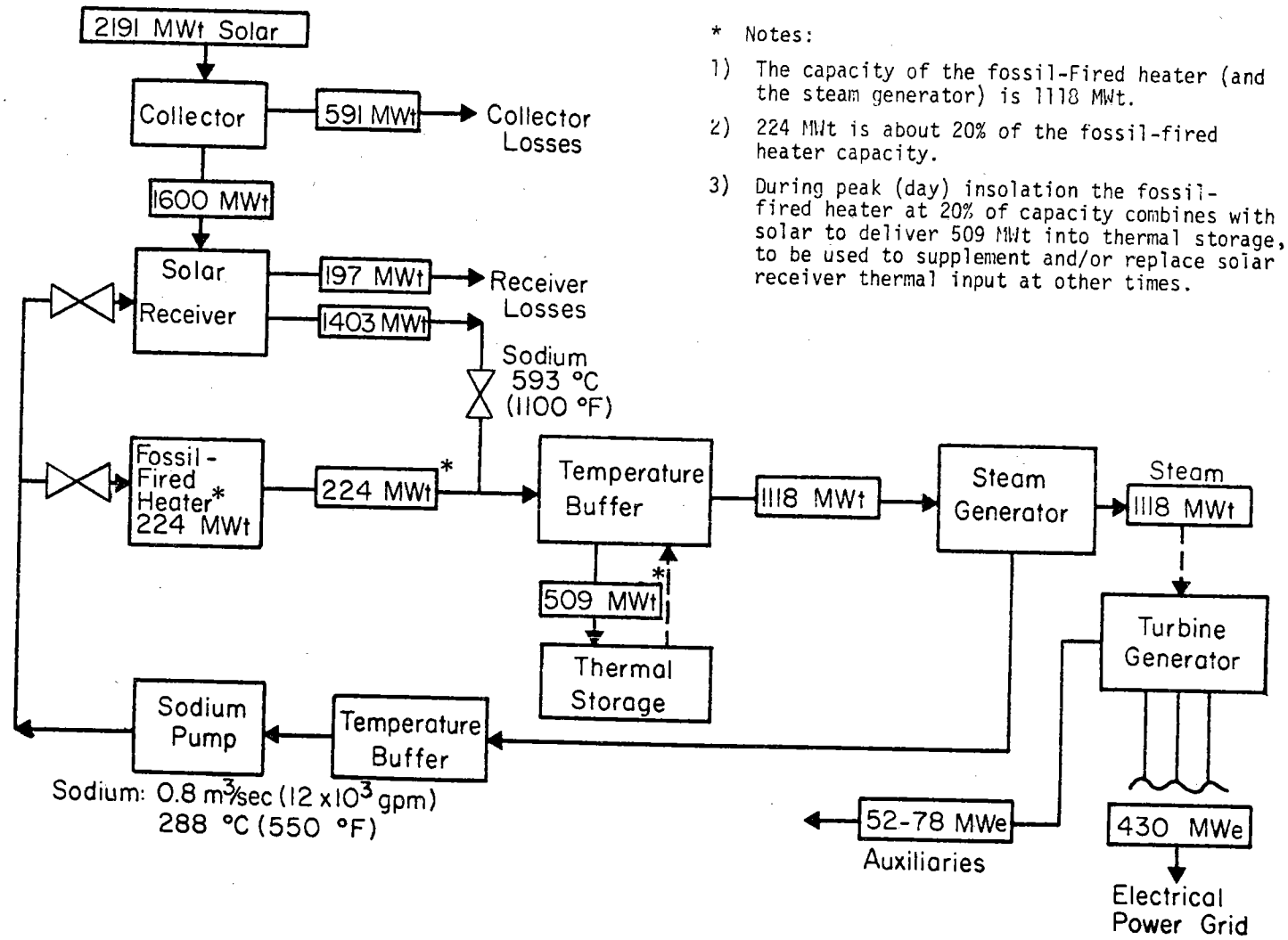

Figure 2-3 Hybrid Plant Power Flow (2.1) (Numbers scaled from Rockwell's figures, and are approximate)

3.0 IMPACT OF EMISSIONS FROM COAL COMBUSTION ON HELIOSTAT PERFORMANCE

3.1 Worst-Case Emissions

The first step in assessing the impacts of emissions from the coal components is to quantify the emission rates of all regulated pollutants. Because any coal-fired power plant would have to meet air quality emissions standards, we will assume that emissions from the proposed plant will take place at the rates established by the standards. This assumption may not be entirely valid for at least three reasons:

- A 430 MW(e) coal burning power plant may not be able to meet the particulate emissions standards established by the South Coast Air Quality Management District using best available control technology (3.1);
- Utilities may control their emissions beyond what is required by the standards, if an emission banking procedure is established;
- Existing emissions standards may not be in effect when the proposed plant is actually operating.

Quantifying the effects of these sources of uncertainties is difficult at the present time.

The Sundesert site is located in Riverside County, and is therefore, under the jurisdiction of the South Coast Air Quality Management District (SCAQMD). Table 3-1 presents the applicable emissions standards for a 430 MW(e) power plant located in the SCAQMD. These data were obtained by multiplying the emissions standards for a 500 MW(e) plant in the same region by 430/500 or 0.86 (3.2).

Table 3-1

Emissions Standards Applicable to 430 MW(e) Coal Power Plant in Riverside County

SCAQMD Rule Number	Pollutant	Maximum Allowable Emissions
405	Particulate Matter	2.9 g/sec (23 lb/hour)
431.3	Sulfur Dioxide	319 g/sec (2530 lb/hour)
475/1135.1	Nitrogen Oxides	92 g/sec (730 lb/hour)
407	Carbon Monoxide	1484 g/sec (11780 lb/hour)

Treating the standards as emissions introduces the additional assumption that the plant will be operating at maximum capacity (430 MW(e)). This is a worst-case assumption, because as discussed in Volume I, the coal portion of the plant is planned to operate most of the time at 20 percent capacity, while the solar component is supplying the remainder of demand. The "worst-case" approach is used frequently in air quality impact analysis; if the worst-case analysis does not suggest undesirable results, one can usually assume that no problem will develop.

Given the emissions from the proposed facility, the next step is to identify which pollutants will impair heliostat efficiency through dry deposition. Wet deposition will not be considered because it would be accompanied by rainfall which would help clean the heliostats and improve efficiency. The emissions in Table 3-1 are either gases or particles when emitted from the power plant stack. Because we are looking only at deposition, we will focus only on particulate matter, assuming the material in the gaseous state will not settle out of the atmosphere or degrade the heliostat surface within the heliostat field. Particulate matter in the plume from the coal stack is composed of secondary particulates formed by chemical reactions between liquid and gaseous aerosols, and primary particulates directly emitted from the stack. The impacts of both types will be discussed.

3.1.1 Secondary Particulates

Some gases (sulfur oxides, nitrogen oxides and hydrocarbons) can react to form secondary particulate matter (sulfates and nitrates) in the atmosphere (3.3). Sulfates and nitrates may be significant if the gas-to-particle conversion occurs quickly enough so that significant amounts of the secondary particles are generated before the power plant plume passes over the outside border of the heliostats. The sulfate conversion process has been extensively studied, with gas-to-particle conversion rates of 0.5 to 2 percent per hour reported; conversion rates can be as high as 10 percent per hour under extreme photochemical conditions (3.4). Particle diameters of atmospheric sulfates have ranged from 0.1 to 5 μm (3.5), which is comparable to the diameters of primary particulates (see the next section).

Dry deposition of particles from the atmosphere onto heliostats is governed by sedimentation and inertial impaction for particles of diameters greater than 1 μm, and by Brownian diffusion for particles with diameters less than 0.1 μm. The deposition velocity is therefore lowest for particles in the 0.1 to 1.0 μm diameter range (3.6).

Some rough calculations can be used to determine if secondary particles will significantly impact heliostat performance. For the purposes of these calculations, the following assumptions are made:

- the coal facility stack is in the approximate center of the heliostat field

- the wind is from the South at 1.6 m/s (3.5 mph) (3.7);
- the heliostat field is approximately round with a radius of 1983 m (13,000 ft) (3.8).

These assumptions are illustrated in Figure 3-1.

At a wind speed of 1.6 m/s (3.56 mph) the sulfur and nitrogen oxides will be out of the heliostat field by the time significant amounts of sulfates and nitrates are formed, even at the 10% conversion rate (which might not be too unrealistic if the volume passes through the solar beam):

$$(1983\ m)/(1.6\ m/s) = 1239s = 0.34\ hours$$

$$(10\%/h\ converison)\ (0.34\ h) = 3.4\%\ conversion$$

The ambient levels of sulfur oxides and nitrogen oxides would thus be only 3.4% converted to particulates as the volume reaches the far edge of the heliostat field. Furthermore, as the plume travels from the stack to the heliostat field, the ambient levels of nitrogen oxides and sulfur oxides become more dilute, as described by the Gaussian diffusion model, thereby reducing the ambient levels of sulfates and nitrates as well. Thus for the purposes of this study, secondary particulate formation will not be considered as a significant source of particulates; only primary particulate matter will be discussed.

3.1.2 Primary Particulates

Assessing the impact of primary particulates on heliostat efficiency through dry deposition will consist of the following steps:

- determine the emission rate and size of emitted particles;
- use dispersion modeling to predict ambient particulate levels reaching the heliostats;
- compute particle deposition rates;
- determine impaired heliostat efficiency based on calculated mass loading.

The proposed facility is assumed to emit particulate matter at a rate of 2.9 g/s (23 lbs/hour). The particulate control technology proposed for the facility is a baghouse or fiber filter. Baghouses exhibit a minimum removal efficiency for particles with diameters in the 0.1 to 1.0 μm range, as shown in Figure 3-2 (3.9).

A simple Gaussian dispersion model will be used to estimate the ambient levels of particulates over the heliostats. The proposed facility is assumed to exist as shown in Figure 3-1, with the coal stack located in the center of the heliostat field. As was discussed previously, this

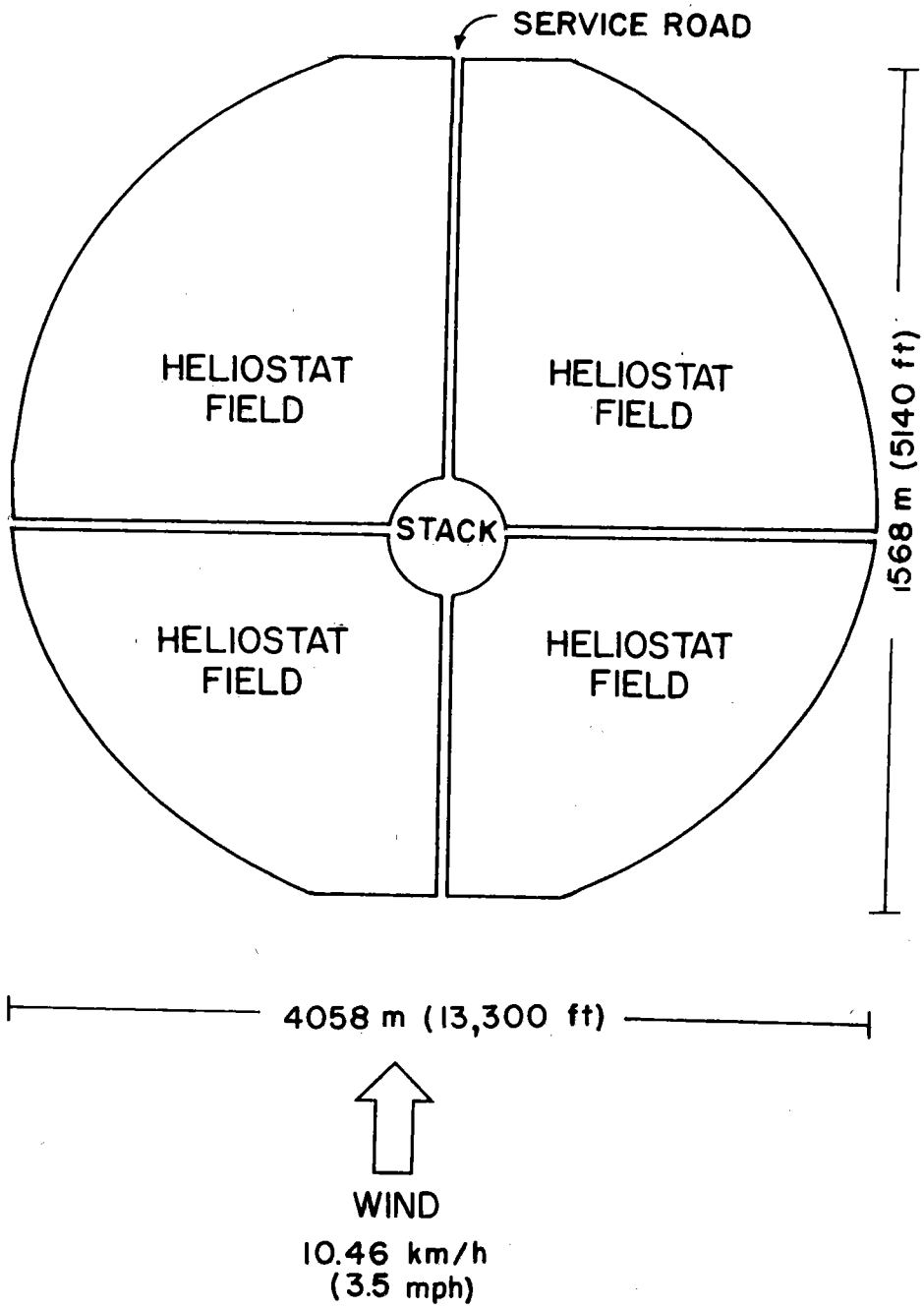

Figure 3-1 Map View of Proposed Facility

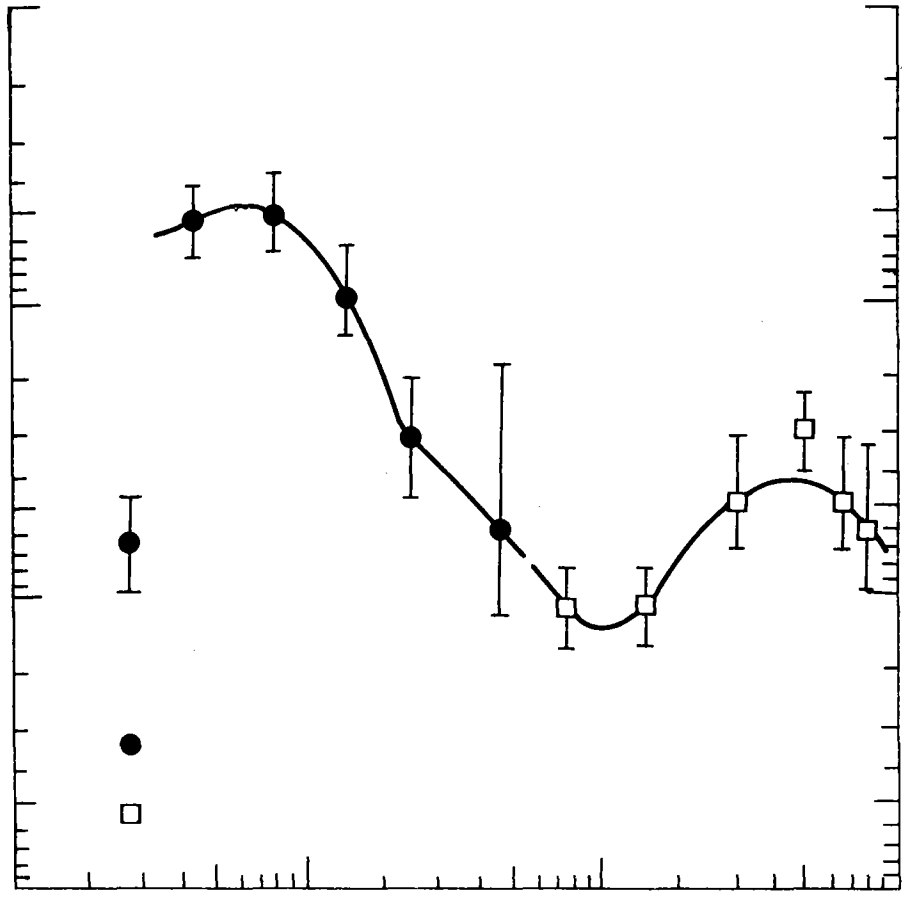

Figure 3-2 Removal Efficiency as a Function of Particle Size for a Fabric Filter Installed on a Coal-Fired Power Plant

layout was selected because it is the proposed design for a 430 MW(e) hybrid plant and because it would represent a worst-case scenario from the standpoint of air quality impacts. The distance from the stack to the edge of the heliostat field is approximately 1980 m (6500 feet). We are therefore interested in determining the width of the plume at 1980 m from the stack, and the ambient concentrations of particulates within that plume at distances from 0 to 1980 m from the stack. Table 3-2 presents the stack parameters that are assumed for the modeling exercise (3.10).

Table 3-2

Stack Parameters

Stack Height	330 m (1083 ft)
Stack Gas Temperature	348.5°K (168°F)
Stack Gas Exist Velocity	35.7 m/s (80.3 mph)
Stack Inside Top Diameter	2.438 m (8 ft)
Stack Gas Volume Flow Rate	162.2 m^3/sec (2.1 x 10^{11} ft^3/hour)
Ambient Temperature	301.1 K (82.6°F)
Ambient Presure	937.9 mb (13.6 psi)

3.2 Worst-Case Meteorology

In addition to specifying worst-case emissions from the proposed facility, worst-case meteorological conditions must also be selected. Three types of meteorological conditions can cause worst-case ground-level ambient concentrations from an elevated source (3.11).

- a turbulent and well-mixed unstable atmosphere (see Figure 3-3a);
- trapping of the plume by the base of an inversion located above the plume stack (see Figure 3-3b);
- fumigation when the plume is emitted into a stable inversion layer and is then entrained into the mixed layer when the inversion is broken up due to surface heating (see Figure 3-3c).

Only the first type of condition is applicable to this study, for reasons discussed in the following paragraphs.

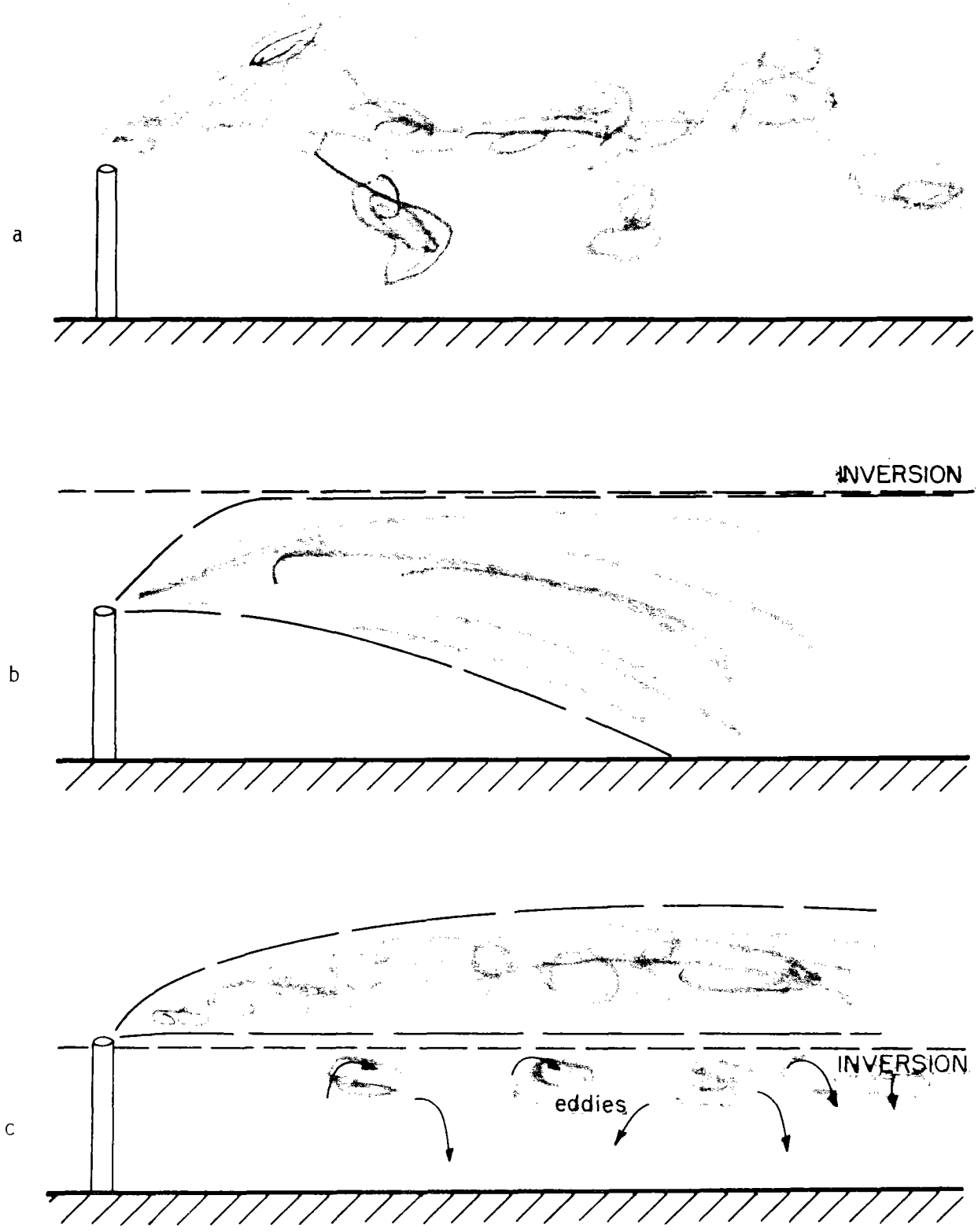

Figure 3-3 Conditions Leading to High Groundlevel Concentrations From an Elevated Source

Elevated concentrations can result when the emissions from an elevated source are trapped beneath a stable layer above an inversion. Vertical dilution of the effluent is inhibited because they can't rise above the base of the inversion. Table 3-3 presents the mean morning and afternoon mixing heights (height of the base of the inversion) in meters for the Blythe site (3.13). The morning mixing heights are so low that, on the average, the stack emissions will go into the inversion layer rather than be trapped beneath its base. The physical stack height itself (330 m) is large enough to exceed mean morning inversion bases for three of the four seasons. The afternoon mixing heights are quite large. The smallest, 1250 m in the winter, would result in trapping at considerable distance downwind. The effects of plume trapping are not apparent until distances greater than $2x_L$, where x_L is the distance at which $\sigma_z = 0.47$ L, and L is the mean mixing height (3.14). For L = 1250, we are interested in the distance at which $\sigma_z = 0.476$ or 500 m, which is approximately 1110 meters distant (x_L). A distance of 2 x_L would be approximately 2300 m, which is almost out of the heliostat field.

Table 3-3

Mean Morning and Afternoon Mixing Heights for Blythe (in meters)

Season	Morning Height (m)	Afternoon Height (m)
Winter	300 (984 ft)	1250 (4104 ft)
Spring	450 (1476 ft)	2200 (7218 ft)
Summer	320 (1050 ft)	2650 (8694 ft)
Fall	330 (1083 ft)	1900 (9234 ft)

Reference 3.13

Worst-case ground level concentrations from elevated sources can also result if the emissions have been released into a stable air layer aloft and fumigation occurs as surface heating erodes the base of the inversion and entrains the trapped pollutants into the mixed layer. These concentrations can last for periods of approximately 30 minutes (3.15). The nearest downwind distance (x) at which fumigation becomes significant (contributes significantly to maximum ground level concentrations), based on the time required to eliminate the inversion, is given by $x = \bar{u}t_m$. In this relation $\bar{u}$ is the mean wind speed in the mixed layer and t_m is the time required to eliminate the inversion from h, the physical stack

height, to h_i, where h_i is the effective stack height plus 2 σ_z (3.16). The value of t_m can be computed with the following:

$$t_m = (h_i^2 - h^2)/4K$$

where: h, h_i are as defined above

K = eddy diffusivity for heat = 3 m^2/sec (3.16).

For our situation an effective stack of 440 m is reasonable, as will be shown in the next section. Using h = 440 m, h_i was computed as 540 m, based on a σ_z of 50 m for F stability (very stable, because it is within the inversion). The value of t_m was computed to be 8200 sec. Using a mean wind speed of 0.9 m/sec, fumigation would not become significant until 7400 m downwind from the stack, at which distance the plume would no longer be over the heliostat field. This is in agreement with a general statement made by Turner that fumigations for large effective stack heights do not become noticeable until 30 to 40 km downwind from the stack (3.17).

From the above analysis we see that the worst-case meteorological conditions to be used in this modeling study will consist of an unstable atmosphere. Pasquill stability class A, the most unstable, will be used for the analysis. It is generally characterized by strong incoming solar radiation and low wind speeds (3.16). Wind speed and atmospheric stability are the two meteorological parameters required to implement Gaussian models. As far as wind speed is concerned, the upper level winds are of most interest because we are concerned with the elevated release of pollutants. From the standpoint of developing a worst-case scenario, we are interested in whatever wind speed is likely to occur at the site that will lead to the highest ground level concentration. In general, the lower the wind speed, the more pollutants that can build up to produce high ground level concentrations. Extensive wind data have been collected at the Sundesert site, and at two levels: 30 feet and 190 feet above the ground. The data taken at 190 feet most closely represent the height of the emissions for our proposed case.

The wind data collected at the site are broken down by stability category, which is determined by wind speed and incoming solar radiation. Generally, six stability classes are reported, A to F, with A being the most unstable atmosphere and F the most stable. As shown previously, we have selected A stability for our worst-case analyses.

The lowest wind speed that was observed at 190 feet at the site under A stability was in the range 1-3 mph (3.18). The midpoint of the range, 2 mph, will be used for the modeling.

3.3 Atmospheric Dispersion Model

A simple Gaussian model was selected for this study for three reasons:

- we are interested in the dispersion of primary pollutants, and therefore we need not address chemical transformations in the atmosphere;
- the terrain within the site is relatively flat, and complex terrain models need not be used;
- we are interested in only one source, so multiple source models are not needed.

Figure 3-4 presents the behavior of the plume as predicted by the Gaussian model. The x axis will be assumed to represent wind from the south, in order to maximize the heliostat area exposed to the plume. The proposed facility is not a perfect circle with the stack and tower in the center; rather, the center is offset to the south (see Figure 3-1). The distance from center to the southern edge is 1568 m, while the distance from center to the northern edge is 2398 m.

The Gaussian model will first be used to predict ground level concentrations on the plume centerline. The full equation used to mathematically describe plume dispersion; with the ground surface acting as a plane of reflection, with release at a height H, and with the point of observation at x, y, z is the following (3.20):

$$\chi = \frac{Q}{2\pi\sigma_y\sigma_z u}\left[\exp\left(-\frac{y^2}{2\sigma_y^2}\right)\right]\exp\left[-\frac{(Z+H)^2}{2\sigma_Z^2}\right] + \exp\left[-\frac{(Z-H)^2}{2\sigma_z^2}\right]$$

which in this instance reduces to:

$$\chi = \frac{Q}{\pi\,\sigma_y\,\sigma_z\,u}\left[\exp\left(-\frac{H^2}{2\,\sigma_z^2}\right)\right] \qquad (3\text{-}1)$$

where:

χ = ground level concentration (g/m^3)

Q = source emission rate (g/sec) = 2.90 for particulates

u = wind speed (m/sec) = 0.90

H = effective stack height (m) = 440

σ_y = horizontal dispersion coefficient (m), a function of downwind distance, x

σ_z = vertical dispersion coefficient (m), a function of downwind distance, x

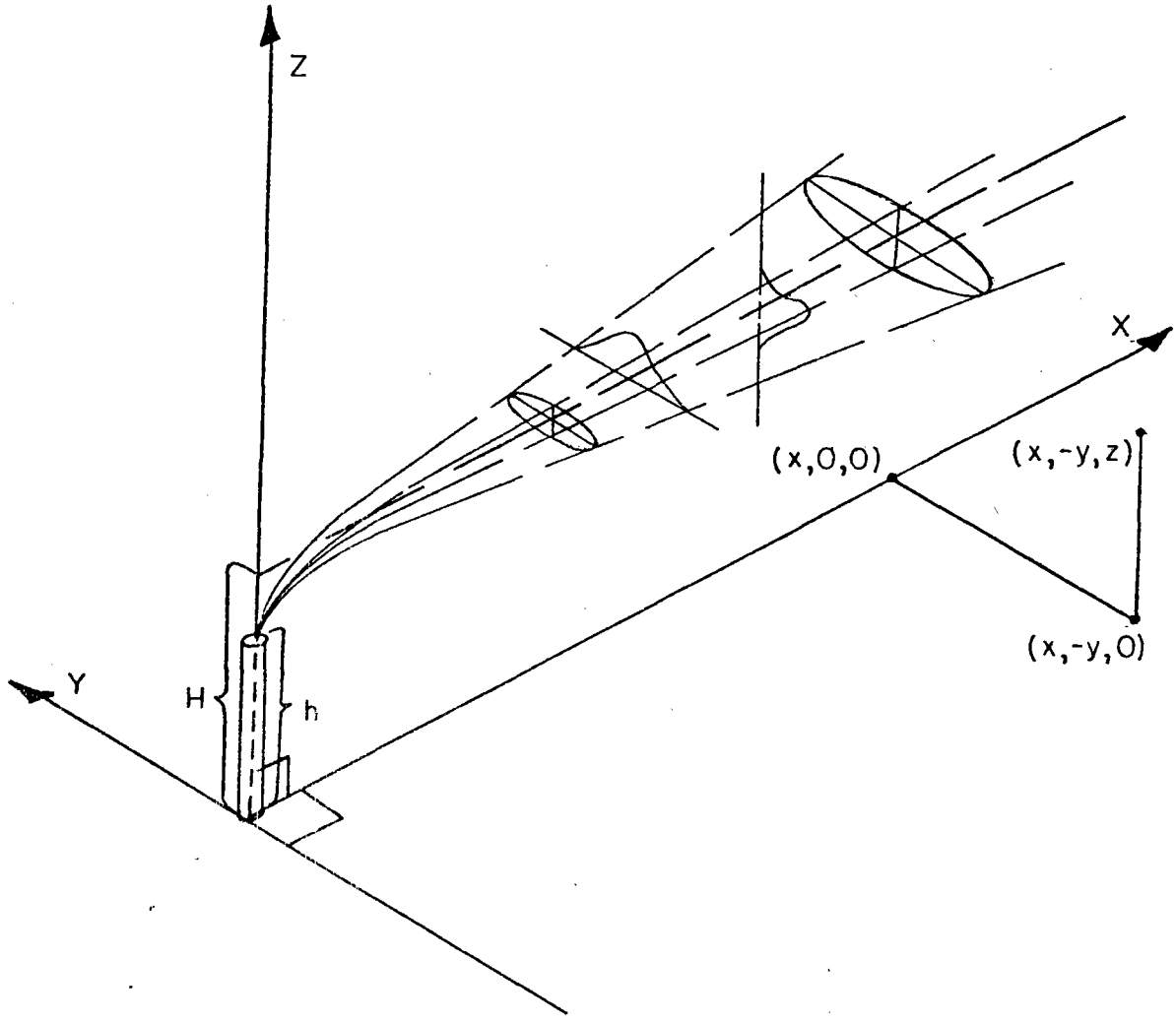

Figure 3-4 Plume Behavior as Predicted by Gaussian Model (Reference 3.19)

The Gaussian model is based upon the following assumptions (3.21, 3.22):

- diffusion in the direction of transport is negligible because it is overwhelmed by wind speed;
- air pollutants are stable inert gases or particles less than 20 μ in diameter which remain suspended in the air over long time periods;
- the equation of continuity if fulfilled:

$$Q = \int_{0}^{+\infty} \int_{-\infty}^{+\infty} \chi u dy dz$$

- none of the material emitted is removed from the plume as it moves downwind, and there is complete reflection at the ground;
- the x-axis is specified by the mean wind direction; a mean wind speed for the diffusing layer can be chosen;
- plume constituents are distributed normally in both the cross-wind and vertical directions;
- the standard deviations (σy, σz) are based on ten-minute averages.

The effective stack height was computed from Holland's equation to be 550 m, as shown in the following calculation (3.23):

$$\Delta H = \frac{V_s d}{u} (1.5 + 2.68 \times 10^{-3} p [\frac{T_s - T_a}{T_s}] d)$$

where:

ΔH = rise of the plume above the stack (m)

V_s = stack gas exit velocity (m/s) = 34.7

d = inside stack diameter (m) = 2.44

u = wind speed (m/sec) = 0.90

p = atmospheric pressure (mb) = 937.9

T_s = stack gas temperature (°K) = 348.5

T_a = air temperature (°K) = 301.1

Substituting:

$$\Delta H = \frac{(34.7)(2.44)}{(0.90)} [1.5 + (2.68 \times 10^{-3})(937.9)(\frac{348.5-301.1}{348.5})(2.44)] = 220 \text{ m}$$

$$H = h + \Delta H = 330 + 220 = 550 \text{ m}$$

The effective stack height of 550 m seems large for a 430 MW(e) power plant, and this might artificially lessen the magnitude of the worst-case impacts. A large effective stack height helps push computed behavior of the plume out over the heliostats, thereby lessening the chances that the plume will impact the ground within the heliostat field. Therefore for the purposes of the atmospheric modeling, an effective stack height of 440 m will be used; 440 m is the average of the effective stack height (550 m) and the physical stack height (330 m). Note that because the mouth of the stack is located above the receiver, and because the receiver will likely generate an updraft due to the focused radiation, the plume could conceivably rise to 550 m before leveling off.

Figure 3-5 presents a map view and Figure 3-6 presents a side view of the plume behavior as predicted by the model under worst-case meteorological conditions as they have been described previously. Note that the Gaussian model also assumes as a worst-case that all particulate matter striking the ground is re-suspended; in effect, completely reflected upward. Thus it is available for impaction on the surfaces of the heliostats. Figure 3-7 illustrates the reflection of particles at the ground level derived from an elevated source (3.20).

Table 3-4 presents σ_z values for downwind distances from 700 m to 2400 m in 100 m increments, together with the value of the reflection factor, and the modified pollutant concentration at each distance assuming an effective stack height of 440 m. The distance intervals of 100 m were chosen because it is the smallest distance for which different σ_z values can be determined from the graphs in reference 3.11. Only the 24-hour concentrations are presented because we are primarily interested in long-term effects. For example, the heliostat washing schedule proposed for the proposed facility is once per month; we are interested in determining what masses of particulates would deposit on the heliostats during this time period. The model as described in equation 3-1 actually calculates only 10 minute average ambient concentrations, because the σ_y and σ_y values are based only on ten-minute sampling periods. To convert the ten-minute concentrations into 24-hour average concentrations, the following equation was used (3.24):

$$\chi_s = \chi_k \left(\frac{t_k}{t_s}\right)^p$$

where:

χ_s = concentration estimate for long sampling time

χ_k = concentration estimate for short sampling time

t_k = short sampling time period = 10 minutes

t_s = long sampling time = 24 hours = 1440 minutes

p = empirical coefficient developed from published dispersion coefficients = 0.17

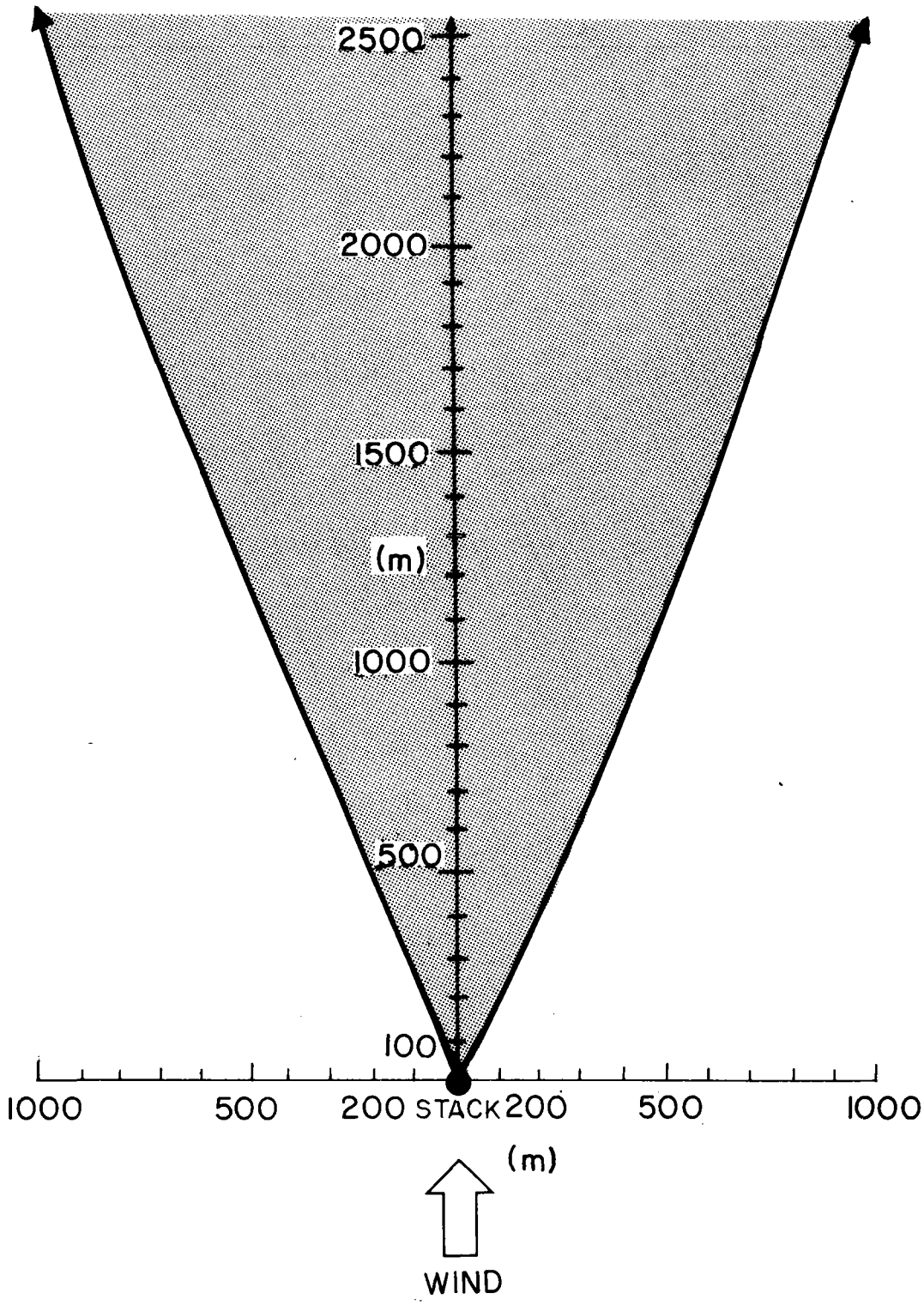

Figure 3-5 Mpa View of Plume Behavior Under "A" Stability

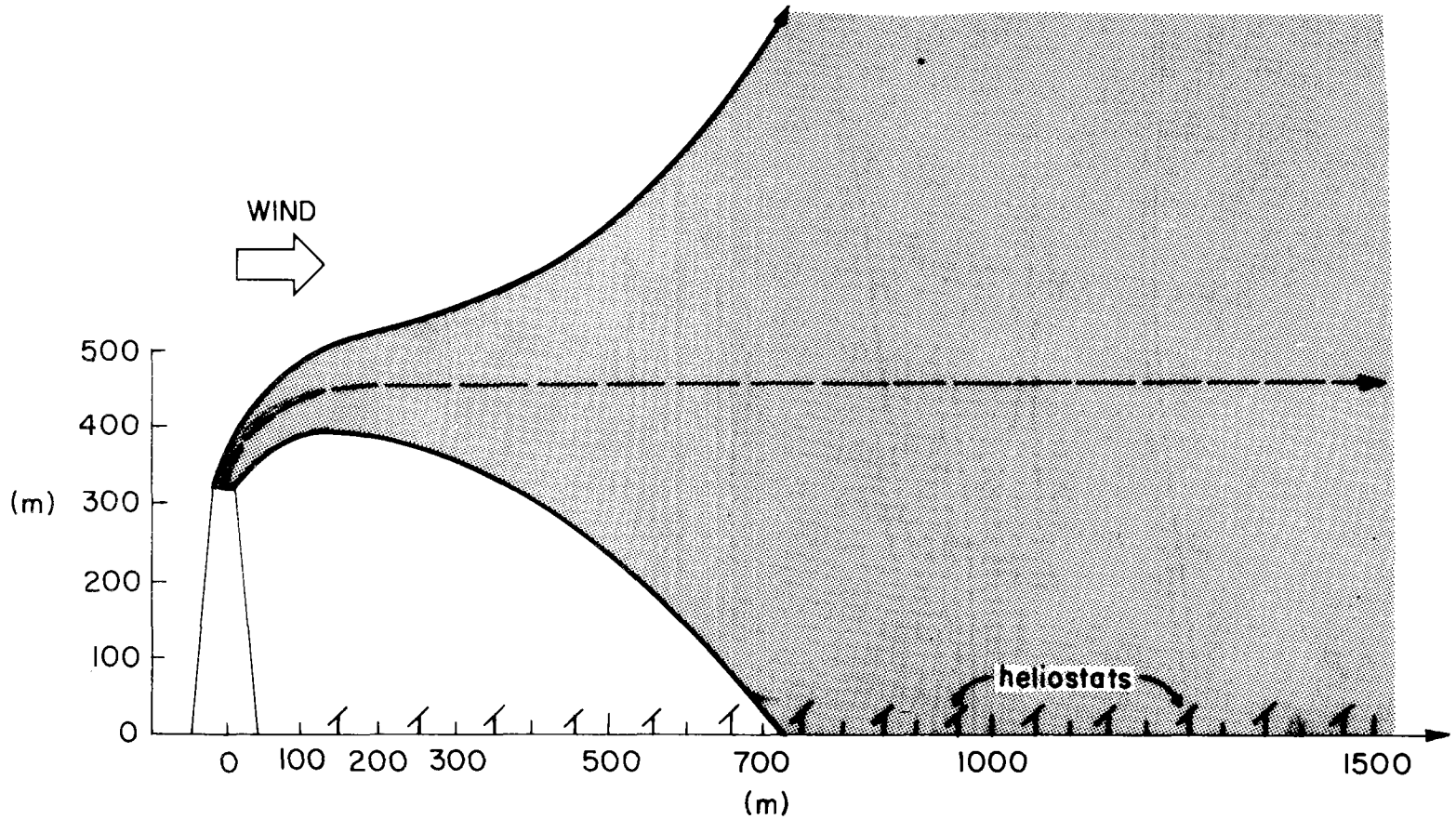

Figure 3-6 Side View of Plume Behavior Under "A" Stability

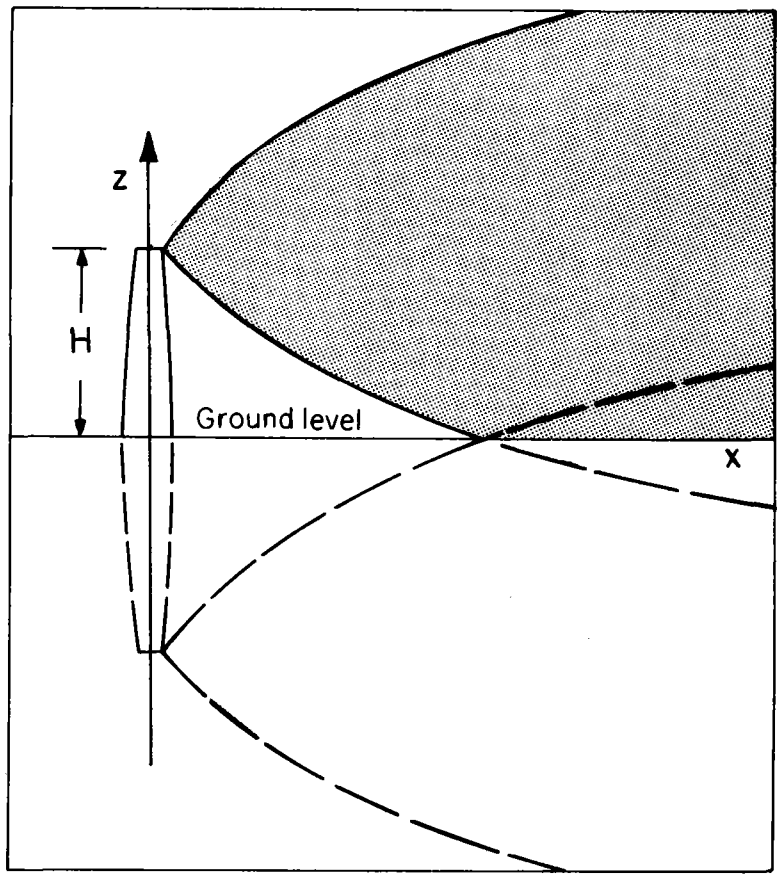

Figure 3-7 Particle Reflection on Ground from An Elevated Source

Table 3-4

Ambient Particulate Concentrations Predicted by Gaussian Model with Reflection

Distance (m)	σ_z (m)	Reflection Factor	24-hour Concentration
700	210	0.223	0.33 ($\mu g/m^3$)
800	290	0.63	1.80
900	360	0.95	2.93
1000	450	1.24	3.48
1100	570	1.48	3.67
1200	790	1.71	3.27
1300	920	1.78	2.79
1400	1000	1.82	2.55
1500	1100	1.85	2.22
1600	1200	1.87	2.02
1700	1400	1.90	1.69
1800	1600	1.93	1.43
1900	1800	1.94	1.20
2000	1900	1.95	1.13
2100	2100	1.96	1.00
2200	2300	1.96	0.86
2300	2600	1.97	0.75
2400	2900	1.98	0.65

Substituting the above values into the equation above produces the following equation for conversion of sampling times:

$$\chi_{24\ \text{hours}} = 0.43\chi_{10\ \text{minutes}}$$

The data in Table 3-4 present estimated particulate levels for the centerline of the plume (x axis in Figure 3-4). Because the plume spreads out as it travels downwind (see Figure 3-5), the ambient particulate levels for various crosswind distances are also needed. The crosswind concentrations are found by multiplying the centerline concentrations predicted at each downwind distance (x) of interest by the Factor $\exp[-(y/\sigma_y)^2/2]$ (3.25). Suitable values of y, the crosswind distance, are chosen for the problem at hand. Table 3-5 presents the estimated crosswind particulate concentrations for various x (downwind) and y (off-center) values of interest.

3.4 Particle Impaction on Heliostat Surfaces

As part of this study, a simple model was developed to estimate the mass deposition rates of suspended aerosols on the surface of the heliostats. Appendix A presents a detailed desciption of the model and the assumptions upon which it is based.

The model can be briefly described as follows. Ambient pollutant levels predicted by a dispersion model are input data. Multiplying the ambient particulate concentration in $\mu g/m^3$ by the ground level wind speed (m/s) produces a particle impaction flux in $\mu g/m^2$-s. This defines the rate of particle impaction on the row of heliostats first contacted by the plume. The impaction rates for heliostats and dispersion than will have reduced the ambient article concentrations. The model assumes (arbitrarily) that 10% of the total mass of particles impacting a heliostat surface stick to that surface, and are thus effectively removed from the air. The ambient particulate concentration at any downwind distance beyond the first row of impacted heliostats (about 700 m downwind from the stack) will thus be 90% of what would have been there without such removal, according to the dispersion model used. In reality, this 10% "sticking coefficient" will most likely not remain constant; rather, it will probably vary depending on wind speed and direction, particle size and chemical composition, temperature, humidity, degree of soiling of the heliostat surface, and other factors. The model also assumed that all heliostats were at a 45° angle from the vertical; in reality the heliostat angle will vary in both space and time.

Figure 3-8 presents the predicted mass of particles that would impact on the entire heliostat surface area within a cell in a 30-day time period (i.e., the cell is treated as one large heliostat). The data have been rounded to express no more than two significant figures. The 30-day time period was chosen because it represents the anticipated heliostat cleaning frequency for the proposed facility. The predicted worst-case particulate deposition, which occurs on the plume centerline in the third row of heliostats was 173 kg per 30-day period. Because the deposition values

Table 3-5

Crosswind Particulate Concentrations Predicted by Gaussian Model at Various Downwind Distances and Crosswind Locations

Downwind Distance = 840 m, χ = 0.92 $\mu g/m^3$

y (m)	y/σ_y	χ(24-hour)
± 370	370/140	0.03

Downwind Distance = 1110, χ = 3.63 $\mu g/m^3$

y (m)	y/σ_y	χ(24-hour)
± 370	370/230	1.00
± 740	740/230	0.02

Downwind Distance = 1480 m, χ = 2.29 $\mu g/m^3$

y (m)	y/σ_y	χ(24-hour)
± 370	370/370	1.10
± 740	740/370	0.12
± 1110	1110/370	0.003

Downwind Distance = 1850 m, χ = 1.32 $\mu g/m^3$

y (m)	y/σ_y	χ(24-hour)
± 370	370/370	0.80
± 740	740/370	0.18
± 1110	1110/370	0.015

Downwind Distance = 2220 m, χ = 0.84 $\mu g/m^3$

y (m)	y/σ_y	χ(24-hour)
± 370	370/400	0.55
± 740	740/400	0.15

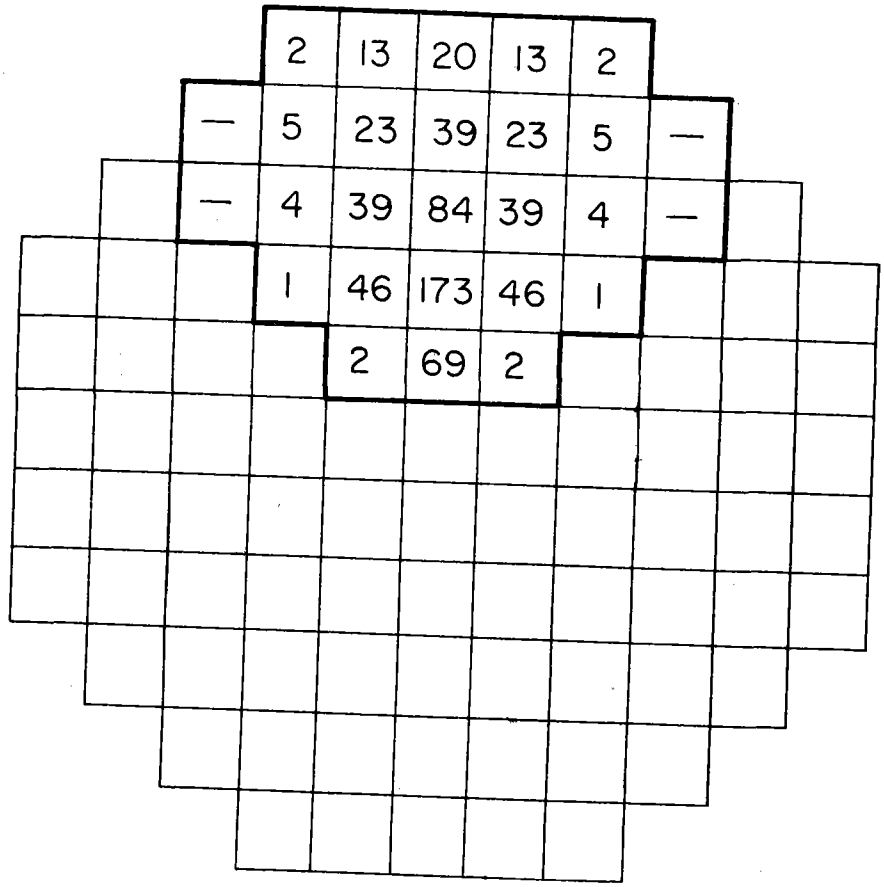

Figure 3-8 Predicted Mass of Particulates Deposited Per Cell Per 30-Day Month

are difficult to visualize on a "per-cell" basis, the data were converted to grams of particulates deposited per heliostat per cell. Figure 3-9 presents these data. The worst-case of 173 kg/30 days translates into approximately 229 grams (about 0.5 pound) per heliostat, which is about 6.5 grams of particulate per square meter area.

3.5 Conclusions and Recommendations for Future Work

The accuracy of the modeling exercise should be discussed before conclusions are drawn so that the results can be interpreted within the proper context. Appendix A presents a complete discussion of the errors associated with the modeling exercise. The most accurate expectation for the Gaussian model is within a factor of three, including uncertainties in σ_z and the mean wind (3.26). Additional uncertainty is introduced into the data shown in Figures 3-8 and 3-9 because of the simplifying assumptions made in the heliostat impaction model. The data in Figures 3-8 and 3-9 should be interpreted to have an uncertainty of about a factor of five, due to the added major sources of uncertainty in the heliostat impaction model.

Considering all the inaccuracies in the model results the data in Figures 3-8 and 3-9 should not be relied on in an absolute sense. Rather, they should be interpreted as a typical concentration field to be expected under worst-case conditions. The most important conclusion that can be drawn from this study is that not all heliostats will need to be cleaned with the same frequency, when considering only emissions from coal combustion.

A heliostat particulate impaction model has been developed. The model predicts that as a worst-case a maximum of 2.29 g might be deposited on a heliostat in a 30-day period. Unfortunately, translating these data into impaired heliostat efficiency will be difficult at best because of the lack of research conducted and results published in this area. Most of the state-of-the-art research in determining the effects of the environment on heliostat performance is not on the quantitative level required by the model; however, it may be possible to use data such as that collected by Sandia Laboratories at Albuquerque.

The data we need for such a study are reflectance degradation as a function of quantitative measures of a physical change for the heliostat; e.g., reflectance as a function of mass loading, reflectance as a function of percent surface covered, etc. Also of interest would be data describing the effects of particles of different sizes and chemical compositions on heliostat performance.

One reason for this lack of data could be that perhaps the best way to determine the impacts of coal emissions on heliostat performance is to perform actual field studies. Considering the inaccuracies in the results of dispersion modeling the mathematically predicted impacts may have little resemblance to reality. It is equally important to remember that a small number of experiments may lead to similar uncertainty. Although

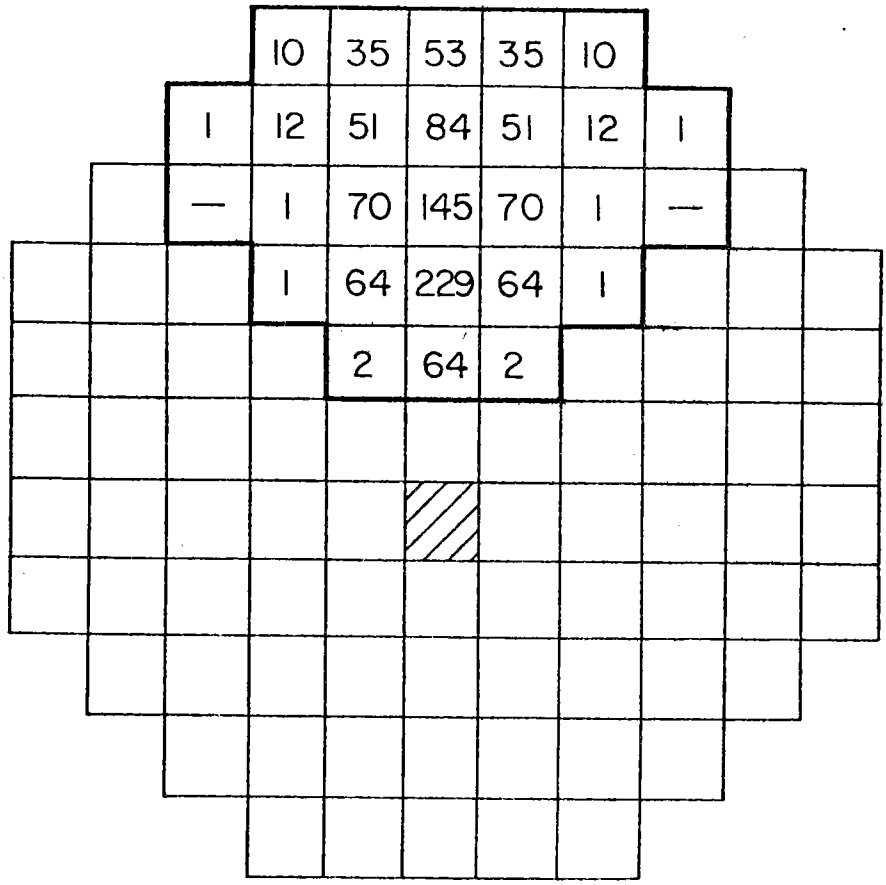

Figure 3-9 Predicted Mass of Particulates Deposited Per Heliostat Per Cell Per 30-Day Month

determining the environmental impacts of a new technology is desirable to do at the planning stage so that appropriate design changes can be made at that stage, some impacts can't be quantified to the extent needed to warrant design changes. A pilot hybrid plant would be desirable so that the effects of coal emissions could be studied over an extended period and various conditions in a real-life-situation.

In spite of this lack of data, a major conclusion that can be drawn from the results of this study is that the amounts of coal particles that could collect on heliostat surfaces are large enough so that the problem requires further detailed study.

Mitigating the worst-case intra-plant air quality impacts can be accomplished by judicious juxtaposition of the emitting subsystems (coal stack, cooling towers) and receiving subsystems (heliostats). A minimum of the heliostat area should be placed downwind of the emitting subsystems along the vector of the prevailing wind; by so doing, most of the time a minimal heliostat area would be adversely impacted by the plume. An extremely effective design change would be to eliminate one quarter of the heliostat field, and increase the number of heliostats in the remaining three quarters to compensate for the loss. The "open" quarter would then be aligned with prevailing winds at the site, and would be placed downwind of the coal stack and cooling towers. Consequently, most of the time emissions would not impact on heliostats. It is important to note that this mitigation measure would only work a given percentage of the days during the year, as described by wind direction frequency data for the site (wind roses). For example, if the prevailing wind blows from the Southwest 80% of the time, then siting the open quadrant to the northeast of the coal stack and cooling towers will mitigate the problem on 80% of the days in a year, on the average. On the other 20% of the days, operation of the solar subsystem may be adversely impacted by emissions from the coal stack and cooling towers.

Natural emissions of dust and aerosols (e.g. vegetable sap and resins) may be of comparable magnitude in terms of absolute amounts of material deposited on the heliostats. The magnitude of the effects of natural emissions will be addressed in Chapter 6.0 of this Volume.

3.5.1 Recommendations

The heliostat impaction model can be refined to produce more accurate results. One area of refinement would be to use more detailed available computer models for the plume modeling. Developing a computer code for the heliostat impaction model is also desirable. The ambient concentrations of particulates could be pinpointed at each heliostat; combining this with the wind data and heliostat angle at each heliostat would allow one to trace the change in concentration in the plume as it moves downwind from the source. A figure for the quantity of particles reentrained into the plume could also be calculated, based on the size and density of the particles and the wind speed on the ground surface. A

detailed analysis of wind flow around the heliostats and particle behavior in that flow is also advisable.

Further research is needed to obtain the data describing impaired heliostat efficiency as a function of some quantifiable physical parameter.

3.6 References

3.1 Southern California Edison Company. "California Coal Project, Notice of Intention," Volume II, Chapter XII. Submitted to the California Energy Commission. NOI Number 79-NOI-3, Table II.B.5.5.1. (December 1979).

3.2 Reference 3.1; data in column entitled "Maximum Allowable Emissions" were multiplied by 430/500 or 0.86. Emissions are proportional to generating capacity. Particulate emissions were rounded to the nearest lb/hour, and the other emissions were rounded to the nearest tens of lbs/hour.

3.3 National Research Council, Committee on Particulate Control Technology, "Controlling Airborne Particles," Published by the National Academy of Sciences, Washington, D.C., page 45 (1980).

3.4 Reference 3.3, page 86.

3.5 Reference 3.3, page 87.

3.6 Reference 3.3, page 90.

3.7 San Diego Gas and Electric Company, "Environmental Report, Construction Permit Stage, Sundesert Nuclear Plant, Units 1 and 2", Volume 2, Figure 2.3-9 (June 1977). The lowest wind speed observed at the nearest station--Blythe--was 0-6 knots. A wind speed of 0 knots wuld not facilitate the desired calculation, so the midpoint of the range, 3 knots, was chosen as a worst-case wind speed.

3.8 Rockwell International, University of Houston, McDonnell Douglas, Salt River Project, Stearns-Roger, Babcock and Wilcox and SRI International, "Solar Central Receiver Hybrid Power Systems, Sodium-Cooled Receiver Concept," Final Report, Volume II,Book 2, Conceptual Design, Sections 5 and 6, Prepared for the U.S. Department of Energy as part of Contract No. DE-AC03-78ET20567 (ET-78-C-03-2233), page 52 (January 1980).

3.9 Reference 3.3, page 65.

3.10 Reference 3.8, Volume III, page 1-12; the stack height for a 430 MW(e) plant was assumed to be 316 m, based on data from this reference. All other stack parameters were assumed to be same.

3.11 Turner, D.B., "Workbook of Atmospheric Dispersion Estimates, " U.S. Department of Health, Education and Welfare, PHSP No. 999-AP-26, page 39 (1969).

3.12 The American Society of Mechanical Engineers, "Recommended Guide for the Prediction of the Dispersion of Airborne Effluents," Second Edition, Edited by the Task Group for Second Edition, New York, (1973).

3.13 Reference 3.7, Volume 2 p. 2.3-5.

3.14 Reference 3.11, page 7.

3.15 Reference 3.11, page 39.

3.16 Reference 3.11, pages 35-36.

3.17 Reference 3.11, page 39.

3.18 Reference 3.7 presents wind speed data by stability class by month for 190 and 33 ft; Table 2.3-142 presents data for July 1974, indicated 8 observations of 1-3 mph at 130 ft under A stability. Because A represents an unstable atmosphere, low wind speeds are not usually found as was the case with many of the months of wind data.

3.19 Reference 3.11, page 5.

3.20 Reference 3.11, pages 8 and 9.

3.21 Reference 3.11, page 6.

3.22 Reference 3.11, page 17.

3.23 Reference 3.11, page 31.

3.24 Reference 3.11, pages 37 and 38.

3.25 Reference 3.11, page 46.

3.26 Reference 3.11, p. 10.

4.0 IMPACT OF SALT EMISSIONS FROM COOLING TOWER OPERATION ON HELIOSTAT PERFORMANCE

Estimating the impacts of cooling tower emissions on heliostat performance will be done using atmospheric modeling work performed for the Sundesert nuclear plant. The approach used to estimate the impact of coal emissions on heliostat performance will not be used here, for the following reasons:

- the Sundesert modeling work provides the data we need--salt deposition rates per unit area for the Sundesert site--with only minor modifications;
- salt particles from the cooling tower plumes are likely to be large enough to be acted upon by gravity.

The cooling towers proposed for the Sundesert plant were expected to meet local emission regulations for particulate emissions for cooling towers; there are no corresponding federal new source performance standards for cooling tower emissions (4.1). Wet mechanical draft cooling towers were proposed for the Sundesert plant. The proposed coal/solar hybrid plant will most likely use wet-dry towers (see Volume I, Section 2.3); however, the assumed use of wet cooling towers represent a worst-case scenario from the standpoint of salt deposition impacts, because the wet towers emit a moist plume which upon evaporation yields salt particles. Two wet cooling towers of the type proposed for the Sundesert plant are estimated to emit salt particles at a total rate (both towers) of 37.5 kg/hour (4.2). A wet-dry tower has no significant amounts of such emissions when operated in the dry mode.

A Gaussian-type model was used to estimate salt deposition rates. The drop concentration, diameter, velocity (horizontal and vertical) and trajectory as a function of time as the drop travels from the top of the cooling tower to the ground were determined by solving a set of simultaneous differential equations as a function of time (4.3).

Finite differences using the Runge-Kutta method were used to obtain the solution (4.4). Figure 4-1 presents an illustration of the method for calculating salt deposition; note the anticipated normal distribution of particles in a cooling tower plume. Note in both Figures 4-1 and 4-2 that the centerline for the salt particles is below the plume centerline, because salt is more dense than the water vapor.

The following assumptions were made in estimating the salt deposition rates (4.7):

(1) Relative humidity of air inside the tower is 100 percent.

(2) Temperature of air inside the tower (from top of drift eliminator to top of tower) remains constant.

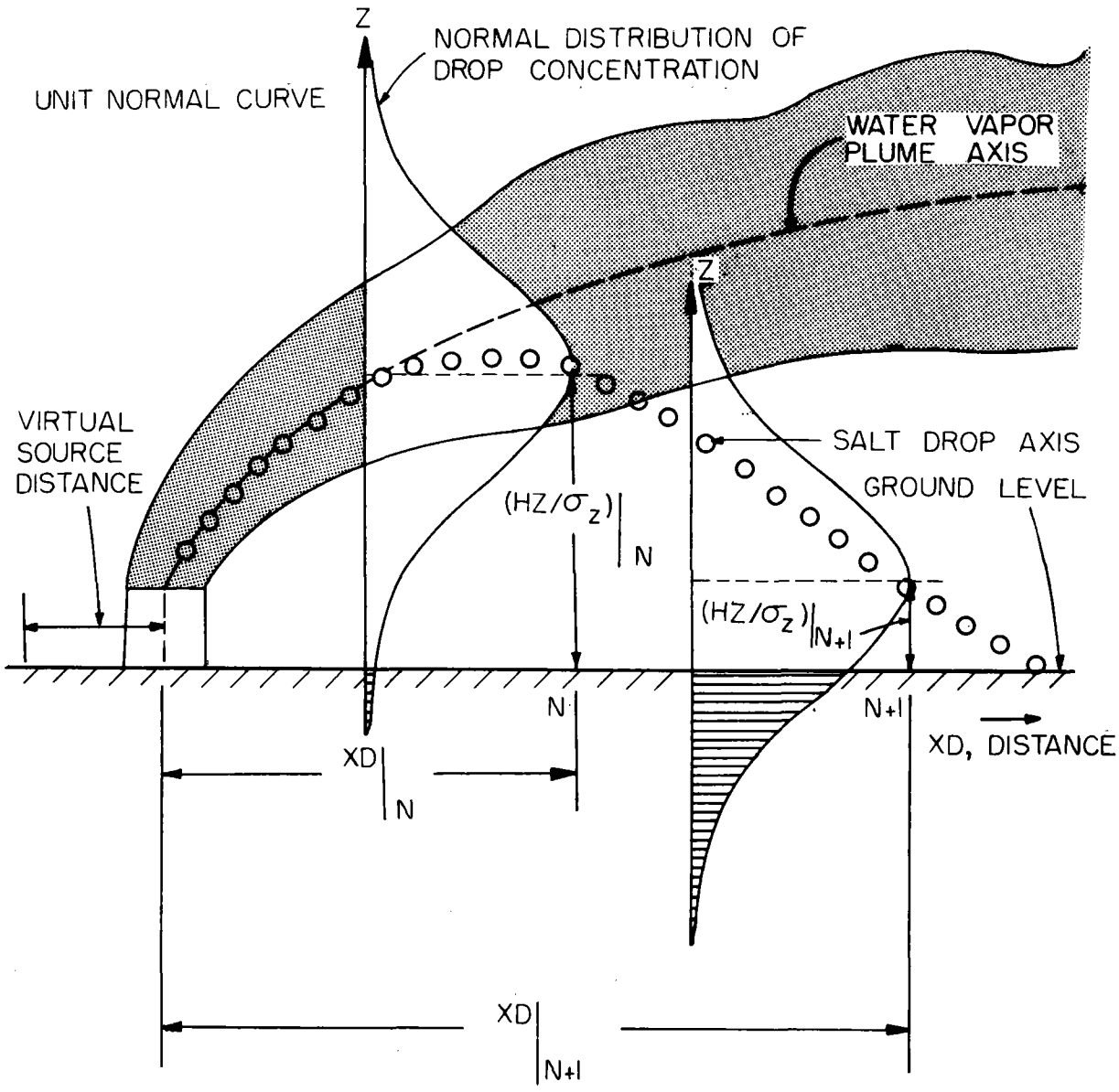

Figure 4-1 Method for Calculating Drift Droplet Deposition
Reference 4.5

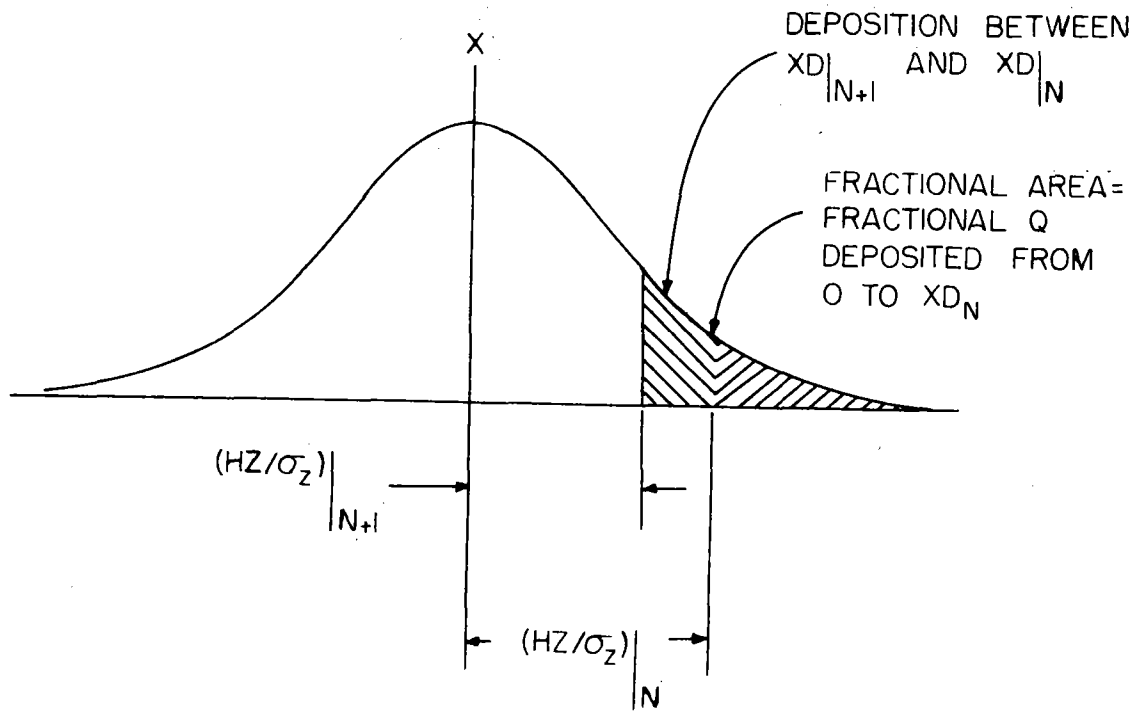

Figure 4-2 Cross Section of Concentration in the Vertical
Reference 4.6

(3) No drop breakup or coalescence occurs.

(4) Inside the tower, the horizontal component of velocity is zero.

(5) Plume relative humidity varies as a function of ambient air relative humidity and downstream distance from the tower.

(6) Plume height is described by Slawson and Csanady's equation for stable low wind speeds (wind speeds $\leq$ 6 mph) and by Brigg's equation for all other conditions.

(7) Plume rise estimates assumed no buoyancy effect due to the release or recovery of latent heat (i.e., only sensible heat has been assumed).

(8) Plume velocity is described by the derivative, with respect to time, of the plume height equation. It applies between the stack exit and XD = 10 HT.

(9) Viscosity, thermal conductivity, diffusion coefficient and Schmidt number remain constant.

Figure 4-3 presents isopleths of salt deposition rates in kg/km^2/month, for the month of July, superimposed on a map of the proposed facility. The data in Figure 4-3 were obtained directly from the Sundesert Report, with the following modifications:

- the location of the cooling towers on the proposed facility was placed at the planned center of the Sundesert facility;

- the values of the isopleths for the Sundesert plant were divided by four to obtain the predicted results for the proposed coal/solar plant; the atmospheric modeling for cooling tower emissions from the proposed Sundesert plant was based on 8 cooling towers; the proposed coal/solar hybrid will have two cooling towers, which is essentially reducing Sundesert emissions by a factor of 4; we assume that total cooling tower emissions from 8 towers are 4 times that for two towers; we also assume that the salt deposition rates are directly proportional to cooling tower emissions, which is reasonable because a Gaussian model was used in deriving the deposition rates; lastly, we are also assuming that the proposed hybrid plant will have identical cooling towers (type, size, etc.) located in the same place as those proposed for the Sundesert plant.

The maximum salt deposition rate predicted by the model is 50 kg/km^2/month for July; this deposition rate is equivalent to 0.05 gm/m^2/month, which is considerably less than the maximum particulate deposition rate predicted for the coal emissions of about 6 gm/m^2/month). Because the data were derived using two different models, different assumptions of plant location and meteorology, their respective results need not agree

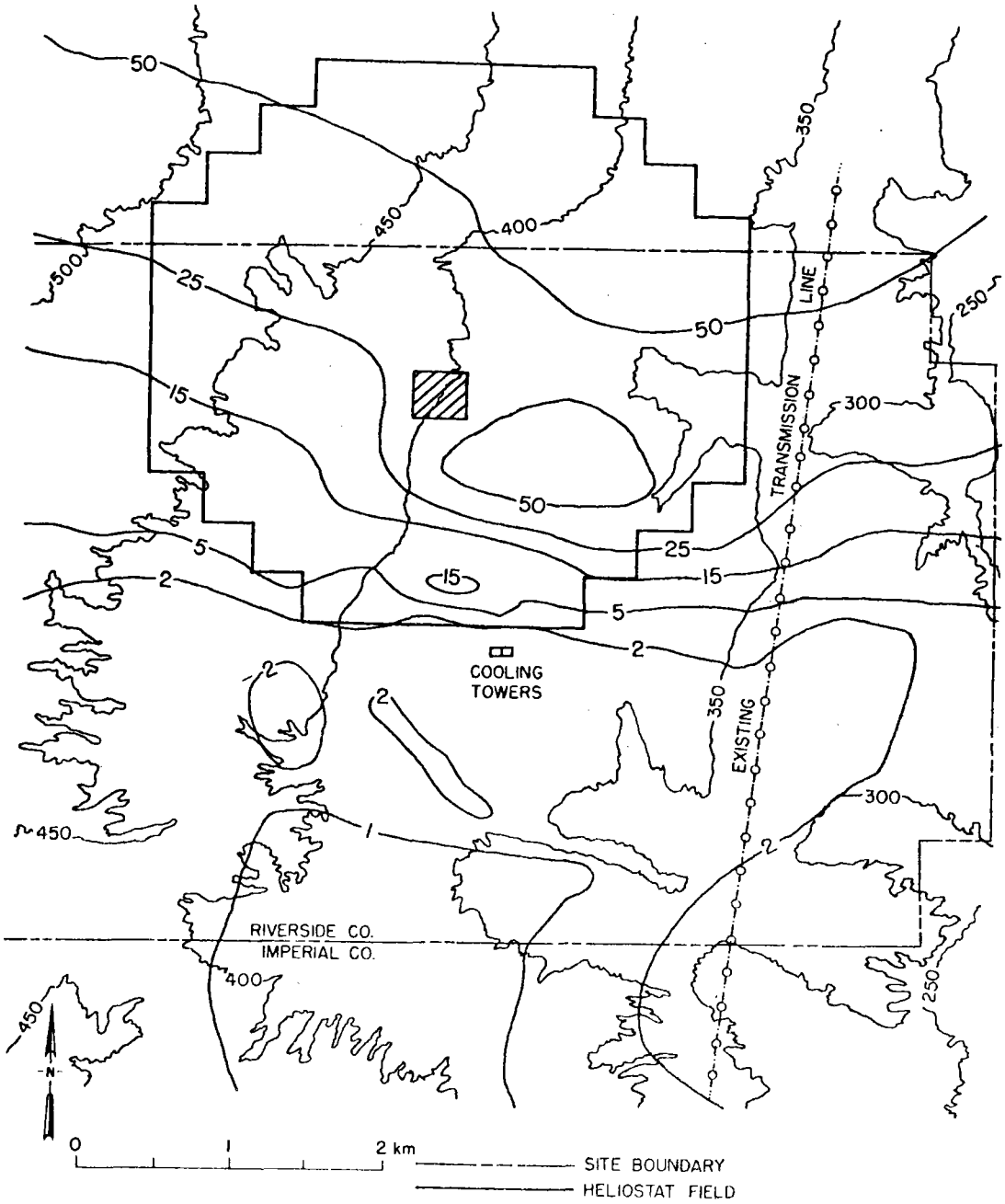

NOTES: DRIFT RATE = 0.002% (75.1 kg SALT/HR/GENERATING UNIT), NUMBER OF TOWERS: 2, EACH HOUR COUNTED AS DRY HOUR

Figure 4-3 Predicted Salt Deposition Rates

exactly. Rather, the data in Figure 4-3 should be used to determine the relative areas of expected high salt deposition rates in the heliostat field. As can be seen the highest salt deposition rates are predicted to occur in the southeast quadrant of the heliostat field; with respect to only salt deposition rates, this area of the field would require a higher cleaning frequency than the other areas.

The modified Sundesert modeling results indicate that two wet cooling towers at the proposed facility will produce salt deposition rates that are insignificant compared to particulate deposition rates. These results do not appear logical when comparing the salt particle emission rates with our computed particulate emission rates. Two cooling towers of the type proposed for the Sundesert plant were estimated to emit approximately 38 kg of salt per hour, which is equivalent to about 11 grams/sec. The emission rate for the particulates from coal combustion was assumed to be 3 g/sec (the emission standard for particulates). Consequently, if an equivalent model were used for both salt and coal particulate emissions, the mass of salt expected to deposit on the heliostat surfaces should be of comparable magnitude to the levels of coal particulates expected. In order to use the heliostat impaction model for salt emissions from cooling towers, one must assume that the salt particles of concern are small enough (less than 1 μ) so that gravity does not influence the deposition. The cooling towers can affect the entire heliostat field, as a worst case (by way of contrast with the coal stack, which only influences half of the field at any given time). Also they would not be expected to produce maximum deposition rates in the same area as the coal emissions. Most likely, the maximum salt deposition rates, as predicted with the heliostat impaction model and assuming a southeastern wind to expose the largest part of the field to the plume, would be in the southern hemisphere of the field. The coal particulate deposition rates reached a maximum in the northern half of the field. Hence the worst-case total particulate deposition rates will likely be averaged out over both halves of the heliostat field, thereby requiring approximately the same cleaning schedules for the entire field.

As was the case in the previous section, we cannot quantify the effects of salt emissions on solar plant performance, because we do not have data describing heliostat efficiency as a function of mass loading of the heliostat surfaces.

4.1 References

4.1 San Diego Gas and Electric Company, "Environmental Report, Construction Permit Stage, Sundesert Nuclear Plant, Units 1 and 2," Volume 4, page 10.1-8 (June 1977).

4.2 Reference 4.1, Volume 2, Figure 5.1-7; the Sundesert cooling towers are assumed to emit 75.1 kg salt/hour per generating unit; since eight towers were planned for two generating units (four towers per unit), then two towers would emit half of 75.1, or about 37.5 kg/hour.

4.3 Reference 4.1, Volume 10, Appendix L, page L2-2-6.

4.4 Reference 4.1, pL.2.2-6, L.2.2-7.

4.5 Reference 4.1, Volume 10, Appendix L, Figure L1.1-4.

4.6 Reference 4.1, Volume 10, Appendix, L, Figure L2.2-4.

4.7 Reference 4.1, Volume 10, Appendix L, p. L2.2-7.

4.8 Reference 4.1, Volume 2, Figure 5.1-7, with modifications as discussed in text.

5.0 ATTENUATION OF INSOLATION BY EMISSIONS FROM THE COAL STACK AND THE COOLING TOWERS

Simultaneous operation of both the coal and solar components of the proposed hybrid plant is likely to occur. At any given time during the day, the coal component will contribute a minimum of 20 percent to the 430 MW(e) output of the plant. Temporary (<3 hours) reductions in available insolation that are expected to last for more than three hours will be replaced by increased operation of the coal component (5.1).

The issue to be addressed here is whether or not operation of the coal component will produce a plume that will reduce the intensity of insolation reaching the heliostats, thereby reducing the contribution by solar components to the total output. Thus, a potential "Catch-22" situation exists: increasing the contribution of the coal component could reduce the insolation available to the solar component, thereby reducing the solar contribution to total output, which in turn requires increased operation of the coal component, etc. At the present time we do not know if hybrid plant operators, faced with a reduced insolation, will elect to shut down the solar component at times and replace it with the coal component, or to operate the solar component at a reduced efficiency and use the coal only as needed.

In order to mathematically predict the loss of available insolation due to operation of the coal component, three tasks need to be performed:

- estimating the ambient concentrations of gases and particles in the plume resulting from coal combustion;
- estimating the reduction in insolation intensity resulting from the gases and particles scattering and absorbing the incoming solar radiation;
- estimating the loss of heliostat efficiency and solar component contribution to total output due to reduction in insolation intensity.

Rockwell performed a plume insolation study for a 100 MW(e) coal/solar hybrid plant to be located in Barstow, California (5.2). The plant is essentially a scaled-down version of the 430 MW(e) used for the environmental assessment in this study. The remainder of this chapter will summarize the Rockwell plume insolation study, and evaluate the study, noting meaningful differences between our plant and the 100 MW(e) plant in the study, and making recommendations for future work in this area.

5.1 Ambient Pollutant Concentrations

The Rockwell study used a Gaussian dispersion model to estimate the concentrations of pollutants in the plume. The basic equation of the dispersion model taken from Turner is given below (5.3):

$$\chi(x,y,z) = \frac{Q}{2\pi\sigma_y\sigma_z u} \exp -\frac{1}{2}\left(\frac{y}{\sigma_y}\right)^2 \exp -\frac{1}{2}\left(\frac{Z-H}{\sigma_Z}\right)^2 + \exp -\frac{1}{2}\left(\frac{Z+H}{\sigma_Z}\right)^2$$

where:

χ = pollutant concentration (g/m^3)

x,y,x = downwind, cross-wind and vertical distances, respectively (m)

u = average wind speed (m/s)

Q = emission rate of pollutant (g/s)

σ_y, σ_z = standard deviations of pollutant plume dispersion for the crosswind and vertical directions, respectively (m)

H = effective stack height (physical stack height + plume rise) (m)

The model thus predicts that within a plume, concentrations will follow Gaussian distributions in the horizontal and vertical directions (see Figure 3-1 for an illustration of Gaussian plume behavior). The paper also lists the assumptions upon which the model is based. The Briggs equation was used in the Rockwell study to calculate plume rise. Figure 5-1 presents the dimensions and layout of the 100 MW(e) plant on which the modeling study is based.

As was discussed previously in this report, air quality impact assessments are ususally based on a "worst-case" approach, in which conditions for the modeling exercise are chosen to maximize computed impacts. Rockwell used this approach in the plume insolation study. From the standpoint of emissions, a worst-case assumption was that the coal furnace was operating at full capacity (100 MWe), thereby producing the operating characteristics shown in Table 5-1 and the emission rates shown in Table 5-2. The worst-case meteorology assumed for the plume modeling study was a wind speed of 2 meters/second under B stabililty. The wind was assumed to be from the south, which would maximize the heliostat area exposed to the plume. These conditions are likely to occur at the Blythe site and will give worst-case predicted concentrations.

The ambient pollutant concentrations predicted by the model were not summarized, because they represent intermediate results that were used in predicting insolation attenuation.

5.2 Pollutant/Insolation Interaction

The gases and particles in the plume emitted from the coal stack can reduce insolation through the processes of absorption and scattering. In the process of absorption, the energy in the insolation is absorbed by the particle or gas and translated into changes in the internal energy levels of the absorbing species; following absorption, the energy can be re-emitted at a different intensity and wavelength. In the scattering process, the energy merely "bounces off" of the gas or particle, and is

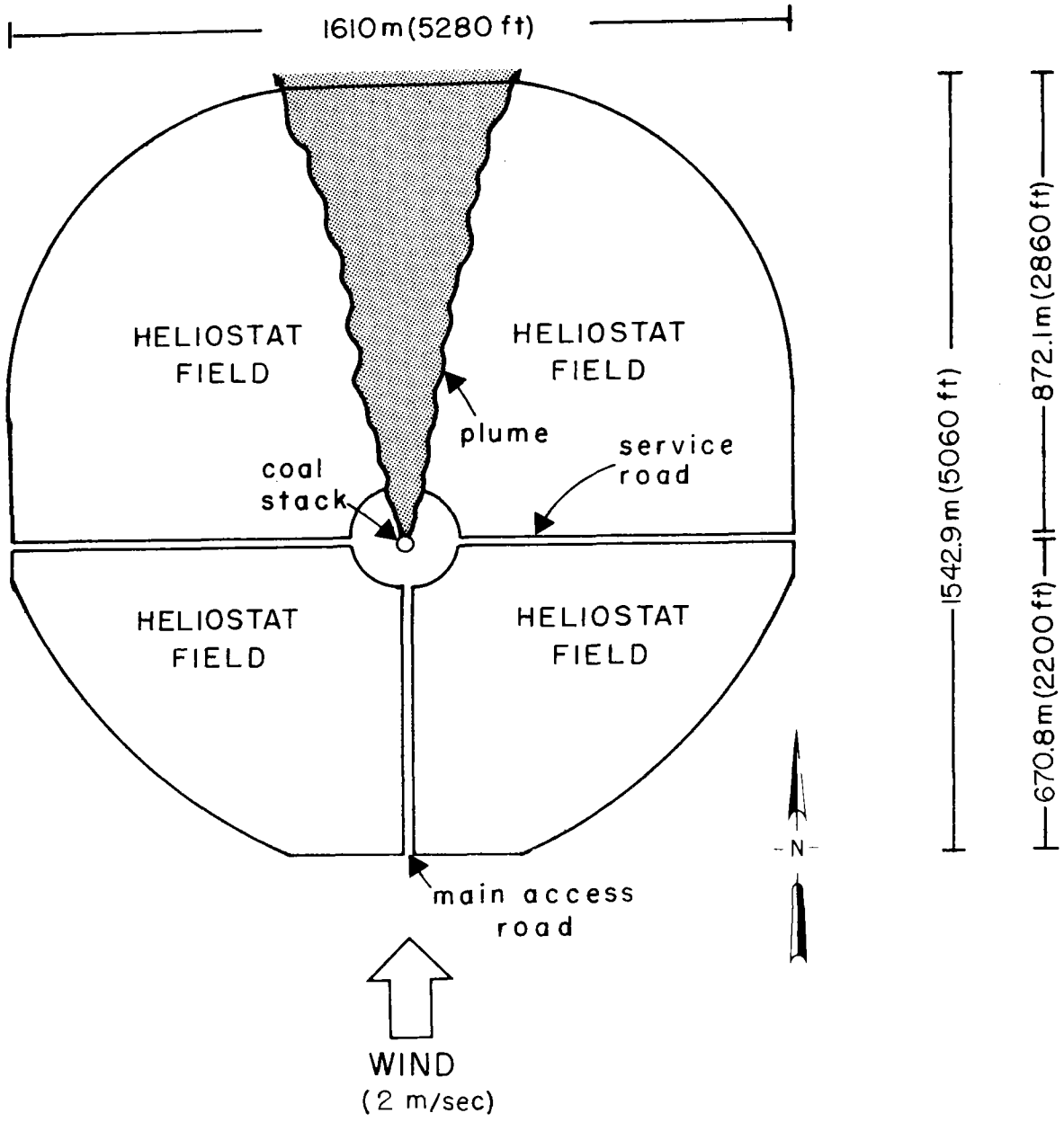

Figure 5-1 Map View of 100 MWe Plant and Meteorological Conditions Assumed for Plume/Insolation Modeling (Reference 5.2)

Table 5-1

Power Plant Specifications
100 MW(e), Full Capacity

Stack Height	137.0 m
Stack Gas Temperature	348.5 k
Stack Gas Exit Velocity	34.7 m/sec
Stack Inside Top Diameter	2.438 m
Stack Gas Volume Flow Rate	162.2 m^3/sec
Ambient Temperature	301.1 k
Ambient Pressure	937.9 mb

Reference 5.2

Table 5-2

Emission Rates
100 MW(e) Coal Plant, Full Capacity

Exhaust Gas Component	Mass Emission Rate (g/s)
N_2	1.028×10^5
CO_2	4.416×10^4
H_2O	8.209×10^3
O_2	8.224×10^3
SO_2	2.379×10^1
Particulates	8.56

Reference 5.2

changed in wavelength and intensity. Both gases and particles can absorb and scatter radiation. However, Rockwell assumed that molecular scattering and particle absorption are not significant processes in attenuating insolation. This is probably valid since particles are not likely to absorb energy because their internal electronic structure is not conducive to energy dissipation; similarly, molecules are more likely to absorb energy than scatter it because they can undergo internal changes in electronic structure.

Beer's Law was used to determine the amount of insolation scattering species:

$$-\sum_i \varepsilon_i c_i l_i$$

where:

I_0 = initial light intensity

I = light intensity at observer

ε_i = extinction coefficient for species i

c_i = concentration of species i

l_i = length of the light path through species i.

For the purposes of this study, the intensity of insolation on top of the plume will be represented by I_0, and the intensity of insolation under the plume and incident upon the heliostats will be represented by I (see Figure 5-2). The ratio of I/I_0 thus gives the fraction of insolation intensity remaining after passage through the plume. The extinction coefficient, ε_i is a measure of how well the particle or gas attenuates radiation. It is a function of both the species and of the wavelength of radiation. For example, molecular nitrogen has a different ε for 1 μ than molecular nitrogen at 5 μ. Furthermore, each species has separate extinction coefficients for scattering and for absorption.

Under carefully controlled laboratory conditions, the concentration c_i can be assumed to be homogeneous within the path length l_i, which is usually accurately defined. When dealing with power plant plumes, however, the concentration c_i changes within the path length (l), as defined by the Gaussian dispersion model. Also, path length changes with distance and is not well defined because the plume does not have explicitly defined boundaries.

In order to minimize the errors resulting from these two factors, Rockwell used the following approach. The combined quantity $(cl)_i$ was calculated for incremental lengths downwind from the stack and then integrated across the plume. The dispersion model was used to estimate ambient concentrations of gases and particles for each incremental cube dxdydz above the heliostat field. The effective value of (cl) was then found through integration:

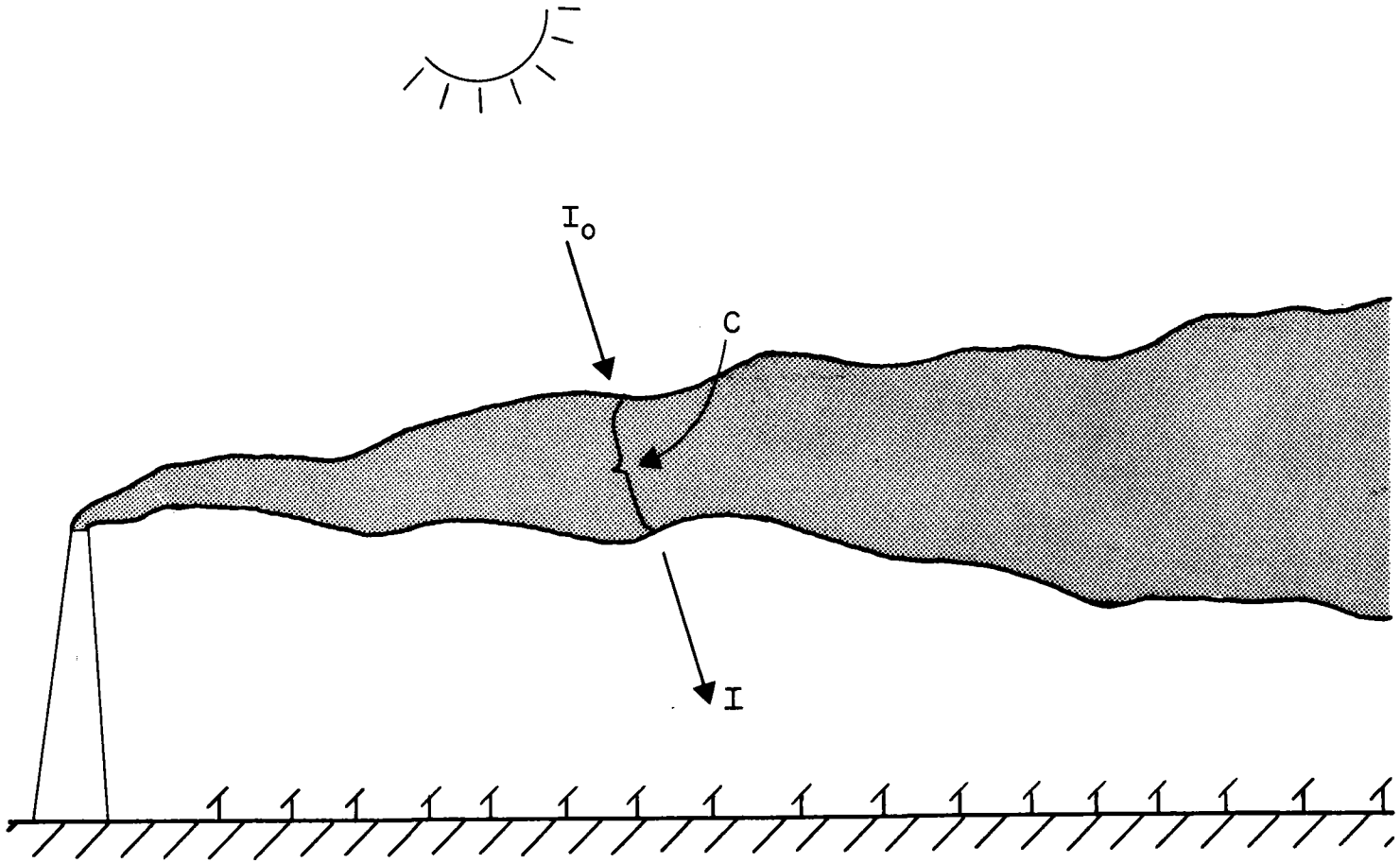

Figure 5-2 Effect of Plume Behavior on Available Insolation As Described by Computer Program "Solar"

$$cl = \frac{\int_{x_{min}}^{x_{max}} \int_{y_{min}}^{x_{max}} \int_{o}^{\infty} \chi(x,y,z)\, dxdydz}{A}$$

where:

x_{min} = radius of small circle surrounding the tower

x_{max} = downwind distance from stack to edge of heliostat field

y_{min} = boundary of heliostat field at x boundary

y_{max} = boundary of heliostat field at center

χ = concentration of pollutant

A = total area of heliostat field.

Numerical integration of the equation was done using a computer program developted by Rockwell entitled "SOLAR." SOLAR uses two subroutines from the EPA dispersion model CRSTR: SIGMA, which calculates σ_y and σ_z as a function of downwind distance from the stack and stability class, and BEH072, which calculates the plume rise using the Briggs equation.

The worst-case emission rates and meteorological conditions discussed previously were used as input to SOLAR. An additional worst-case assumption was that the sun is due south of the tower at 56° from horizontal (Barstow latitude is approximately 34°) so that mid-day conditions are modeled.

SOLAR was used to calculate a value for (cl), this was done using the dispersion equation and other subroutines for sun angle change, etc. Instead of running SOLAR for with an assumed emission rate of 1 g/s, each pollutant, it was run with an emission rate of 1 g/s, under B stability with a wind speed of 2 m/s. The value of (cl) obtained was 2.30×10^{-4} g/m^2. To obtain a (cl) value for each pollutant $[(cl)_i]$, which is needed for Beer's Law, the (cl) value was factored according to the mass emission rate of each species 1 (Table 5-2). The extinction coefficients, ε_i, were obtained from the literature for each species. Again, only molecular absorption and particle scattering were considered, so only ε's for these processes were obtained. Scattering coefficients for particulate matter are less well-defined in the literature than molecular absorption coefficients. For particles, ε is a function of both the particle size and of the wavelength of radiation being scattered. The maximum value of for visible radiation is for particles with diameters of 0.5 μ. Therefore, as a worst-case assumption, all particles were assumed to have a diameter of 0.5 μ, a density of 1 g/m^3, and an extinction coefficient that varies with wavelength according to the following equation:

$$\varepsilon = 14.2\, e^{-\lambda}$$

where ε is in m^2/g and λ is in μ. In addition, all scattered light is assumed to be scattered out of the heliostat field, another worst-case assumption.

Given the values for $(cl)_i$ and ε_i, Beer's Law was used to estimate the value of I/I_o, by summing the $\varepsilon_i(cl)_i$ values for all gases and particles for both scattering and absorption processes. Table 5-3 summarizes these data, the total reduction in radiation resulting from absorption and scattering by all gases and particles. The ratio of I/I_o can be thought of as the percentage reduction in available insolation reaching the heliostats. For example, an I/I_o ratio of 0.741 means that the intensity of the insolation reaching the heliostats is aboout 74% of the intensity of the insolation incident to the top of the plume. As can be seen, the data suggest that the plume has a minor effect on available insolation at most wavelengths. The data can be attributed to the various species emitted by the coal plant in the following manner:

- below 2 μ, light scattering by particles is the dominant process reducing insolation; this study indicates that particle scattering is not important;
- above 2 μ, absorption by water vapor becomes significant, contributing about 10% to the total reduction at 2.5 μ and increasing to 50% at 5.0 μ;
- molecular nitrogen, oxygen and sulfur dioxide do not contribute significantly to the reductions at any wavelength;
- the greatest reduction in insolation, which occurs at 4.2 - 4.4 μ and around 2.7 - 2.8 μ, is due to molecular absorption by carbon dioxide.

5.3 Conclusions and Recommendations

The overall technical approach used by Rockwell is well designed and should be given further consideration and study. The data in Table 5-3 should not be interpreted as the actual insolation reductions that could be expected to occur at the Blythe site with the proposed 430 MW(e) hybrid plant. Consequently, the Rockwell approach should be repeated, using worst-case plant emissions and meteorological conditions applicable to the proposed site and facility, with the following further changes.

The primary change that should be made in the model is that the equation for calculating (cl) should be modified to properly account for the area expected to be covered by the plume, and concentrations intercepted along a path through the plume. Given the stack and meteorological conditions, the plume profile could be defined. From the profile, the area under the plume could be estimated. For the proposed facility, under A stability and a wind speed of 1 m/sec, the area covered by the plume represents approximately 20% of the total area in the heliostat field.

Table 5-3

Transmittance vs Wavelength

$\lambda(\mu)$	I/I_o	$\lambda(\mu)$	I/I_o
0.35	0.981	2.5	0.997
0.40	0.982	2.6	0.996
0.45	0.982	2.7	0.923
0.50	0.983	2.8	0.935
0.55	0.984	2.9	0.964
0.60	0.985	3.0	0.998
0.65	0.986	3.1	0.998
0.70	0.986	3.2	0.998
0.8	0.987	3.3	0.999
0.9	0.989	3.4	0.999
1.0	0.990	3.5	0.999
1.1	0.991	3.6	0.999
1.2	0.992	3.7	0.999
1.3	0.992	3.8	0.999
1.4	0.993	3.9	0.999
1.5	0.994	4.0	0.999
1.6	0.994	4.1	0.999
1.7	0.995	4.2	0.879
1.8	0.995	4.3	0.741
1.9	0.996	4.4	0.796
2.0	0.996	4.5	0.953
2.1	0.997	4.6	0.999
2.2	0.997	4.7	0.999
2.3	0.997	4.8	0.999
2.4	0.997	4.9	0.999
		5.0	0.999

The Rockwell method of dividing by the total area does not give a worst-case impact; the (cl) values are artificially lowered. This does not represent a worst-case scenario, nor does it realistically represent an actual situation. One would expect only the heliostats under a plume to be significantly affected by the plume.

A second major deficiency in the study is that no conclusions were drawn regarding the effect of the reduction in insolation on heliostat performance and overall plant performance. The results given in Table 5-3 are of little value in estimating the impact of the coal component operation on the solar component operation, unless accompanied by data describing heliostat performance as a function of radiation intensity at each wavelength. In addition, data describing solar component output as a function of heliostat performance are needed. For example, studies at Denver have shown that a 25% change in insolation will cause a 40% change in annual energy collection (5.5). Data such as these are needed to complete this study.

The Rockwell study also ignored particulate (salt) and water vapor emissions from the cooling towers. The SOLAR program should be run using the estimated salt and water vapor emission rates from the cooling towers.

Another deficiency in the study was that the pollutants carbon monoxide (CO) and nitrogen oxides (NO_x) were not considered. The absorption spectra of these pollutants need to be examined to obtain the extinction coefficients. Nitrogen dioxide (NO_2) is known to be a strong absorber of ultraviolet radiation, because NO_2 photodissociation is an initial step in the photochemical smog reaction (5.6). In addition, primary pollutants such as ozone and sulfates can affect the intensity of radiation reaching the heliostats; ozone in particular has been shown to be an absorber of ultraviolet radiation (5.6).

5.4 References

5.1 Rockwell International, University of Houston, McDonnell Douglas, Salt River Project, Stearns-Roger, Babcock and Wilcox, and SRI International, "Solar Central Receiver Hybrid Power Systems, Sodium-Cooled Receiver Concept," Final Report, Volume II, Book 1, Prepared for the U.S. Department of Energy as part of Contract Number DE-AC03-78ET 20567 (ET-78-C-03-2233), pages 239-274 (January 1980).

5.2 Reference 5.1, Volume III, pages L4-L17.

5.3 Turner, D.B. "Workbook of Atmospheric Dispersion Estimates," U.S. Department of Health, Education and Welfare, PHSP No. 999-AP-26, page 5 (1969).

5.4 Reference 5.1, Volume II, Book 1, pages 239-274.

5.5 Bird, R.E. and R.L. Hulstrom. "Aerosols and Solar Energy," Solar Energy Research Institute, Paper Presented at the Workshop on Artificial Aerosols, Sponsored by the Institute for Atmospheric Optics and Remote Sensing, and the Naval Research Laboratory, The Antlers, Vail,Colorado, SERI Report Number TP-36-309, Microfiche (June 19-20, 1979).

5.6 Peterson, J.T. and E.C. Flowers. "Interactions Between Air Pollution and Solar Radiation," Solar Energy, 19:23 (1977).

6.0 IMPACT OF FUGITIVE AND NATURAL EMISSIONS ON THE SOLAR SUBSYSTEM

The preceeding three chapters of this volume have discussed the impacts of the coal combustion and cooling tower subsystems on the solar subsystem. A fourth topic that needs to be addressed is the potential impact of fugitive and natural emissions on plant operation. If the emissions from these sources are of comparable magnitude to those generated by the plant subsystems, then a potentially difficult problem exists, because the emission sources can be difficult to control. Fugitive emissions are defined as those that are not discharged to the atmosphere in a confined flow stream (6.1). The most significant fugitive pollutant in a desert environment is particulate matter, usually referred to as fugitive dust. Natural emissions, as their name implies, are those that result from processes not resulting from man's activities. Typical natural emissions are organic gases and particulates given off by vegetation, water, blowing sand, etc. At times the distinction between fugitive and natural emissions is difficult to discern; for example, a short-term impact of a vehicle traveling on a desert road is the production of fugitive dust. A long-term impact may be that the vehicle has exposed more fine material to wind action so that natural emissions have increased.

This section will examine the impacts of the plant on itself, the environment on the plant and the plant on the environment, as related to the production of fugitive and natural emissions. Not all topics are covered in sufficient depth to allow finalization of impacts; therefore, recommendations for future work are discussed where appropriate. The primary issue of concern is whether or not fugitive or natural emissions or both can significantly impair heliostat performance through deposition or impaction.

6.1 Fugitive Dust Emissions Outside Plant Boundary

One issue of concern is the impact of fugitive dust emissions from desert traffic on heliostat performance. Studies have shown that fine particles in a desert environment will collect on heliostat surfaces even when the heliostats are turned face down (6.2). Consequently, when the heliostats are face up, larger particles are likely to collect on the heliostat surfaces, in addition to the fine particles.

As a result of these observed phenomena, natural dust in the desert is likely to collect on heliostat surfaces at the proposed facility. The problem can be aggravated by man's activities, which generate fugitive dust and also alter the environment so as to increase natural emissions. Specifically, the widespread use of off-road vehicles (ORV's) is a potentially significant source of fugitive dust, and could therefore potentially have a significant impact on the operation of the solar subsystem. The only feasible way of controlling the problem is establishing a plant exclusion area; i.e., fencing off an area that is large enough so that any dust generated by vehicular activity in the desert would settle out of the air before reaching the heliostat field. The problem is further complicated by the fact that the hybrid plant will likely attract

people because of its appearance and uniqueness. Therefore, an issue of interest is the size of the exclusion area that is necessary to mitigate the impacts of ORV operation.

Quantifying the impacts of ORV operation on heliostat efficiency is difficult at best because of many complicating factors; e.g., vehicle size, vehicle type, speed, location, meteorology, etc., all influence the impacts of ORV operation on heliostat performance. In addition, the data gap discussed previously--lack of quantitative descriptions of heliostat efficiency as a function of mass deposition--prevents final quantification of the impacts.

As was done previously, a worst-case approach will be used in estimating impacts. A number of simplifying assumptions must be made in order to estimate the impacts. Worst-case assumptions will be used, and the validity of those assumptions may magnify the uncertainties of the results.

6.1.1 Worst-Case Emissions

The first step in estimating fugitive dust impacts of ORV operation is to compute a fugitive dust emission factor. An applicable formula for such a factor (EF) is the following (6.3):

$$EF = 5.9\left(\frac{s}{12}\right)\left(\frac{S}{30}\right)\left(\frac{W}{3}\right)^{0.8}\left(\frac{d}{365}\right) \text{ lb/VMT} \qquad \left(VMT = \begin{matrix}\text{Vehicle Miles} \\ \text{Travelled}\end{matrix}\right)$$

where:

s = silt content of road = 25% for dirt road (6.4)
S = average vehicle speed = 40 mph (assumed)
W = average vehicle weight = 1 ton (6.5)
d = # dry days per year = 345 (6.6)

Substituting the above values into the equation produces a worst-case emission factor of 6.43 lbs/vehicle mile traveled (VMT).

In order to use the model, emissions data must be converted to a fugitive source emissions rate. For the purposes of this study we will consider the ORV's to be a ground-level line source at the north edge of the heliostat field. Assuming the wind to be from the north will expose the greatest part of the heliostat field to the emissions, and thus represents a worst-case situation. Converting the emissions factor to a line-source emissions rate was done using the following equation:

$$Q = \frac{(EF)\ (S)\ (V)\ (f)\ (7.83 \times 10^{-5})}{L} \text{ g/m - sec}$$

where:

EF = emission factor = 6.43 lb/VMT

S = average vehicle speed = 40 mph

V = number of vehicles = 10 (assumed)

f = fraction of miles traveled within effective line source length = 0.1

L = effective line-source length = 3.2 miles (assumed)

It is expected that RV's may operate for a typical 8 hour period each day, but only a fraction of the total distance traveled will be within the line-source element adjacent to the field of heliostats and so of concern. Substituting these values into the above equation produces an emission rate of 6.30×10^{-3} g/m-sec.

6.1.2 Worst-Case Meteorology

Meteorological conditions expected to produce maximum ground-level concentrations from ground-level sources are a stable atmosphere and low wind speed (6.7). The most stable atmosphere considered by Turner, Pasquill Class F, has been reported to occur at the site. The lowest ground-level wind speed associated with that class is 0.9 m/s (6.8).

6.1.3 Atmospheric Modeling

An appropiate model for predicting ambient concentrations in this situation is the following (6.9):

$$\chi = \frac{2Q}{(\sqrt{2\pi})\ \sigma_z u}$$

where:

χ = ground level ambient concentration, g/m^3

Q = source strength in g/m-sec

σ_z = vertical standard deviation of plume (see section 3.3 for a description of the model)

u = mean surface wind speed = 0.9 m/s

The χ values predicted by the model must be further adjusted for the fraction of total emissions that remain suspended, and for averaging time. According to recent data, 32 percent of those particles emitted from dirt roads will remain suspended indefinitely and will thus be available for deposition of heliostat surfaces (6.10). The χ values must also be adjusted for sampling times; 24-hour χ values are computed with the following relationship (see Chapter 3.0):

$$\chi_{24\text{ hours, fine}} = (0.43\ \chi_{10\text{ minute, total}})^{(0.32)}$$

Figure 6-1 illustrates the assumptions used in the modeling study. Two exclusion areas were chosen for analysis: circles of 1 mile and 2 mile

distances beyond the border of the heliostat field. Circles larger than 2 miles were not addressed because of the tremendous area required by the plant and exclusions area (see Volume I, Chapter 4).

Table 6-1 presents the 24-hour ambient fugitive dust levels predicted by the model for various distances at a one mile exclusion area, and Table 6-2 presents the same data for a 2 mile exclusion zone. The predicted χ values are greater in magnitude to the values predicted from coal emissions.

Once the χ values are obtained, the heliostat particle impaction model described in Appendix A will be used to predict the mass of fugitive dust deposited over a period of time on the heliostats, with the source effective 8 hours out of a 24-hour day.

$$M = (\chi)\ (u)\ (S)\ (A)\ (N)\ (8.64 \times 10^{-4})$$

χ = ambient particulate concentration predicted by the Gaussian model ($\mu g/m^3$)

u = mean wind speed in the 20 m boundary layer (m/s)

S = sticking coefficient; the fraction of particles remaining on the heliostats after they have impinged upon the heliostat surface

A = cross sectional area of the heliostat (m^2)

N = number of heliostats/cell

2.59×10^{-3} = constant to convert results to kg deposited per 30-day month

M = predicted mass of particulates deposited per 30 day month

Figures 6-2 and 6-3 present the predicted mass of fugitive dust (kg) deposited per heliostat cell in a 30-day period for 1- and 2-mile exclusion areas, respectively. While these represent a nominal worst-case for RV-generated fugitive dust emissions, it is conceivable that this kind of source--highly variable--could be ten times as large. It certainly is unlikely to be unimportant. These data should not be used to select an appropriate exclusion areas until data describing impaired heliostat efficiency as a functioin of mass loading of the heliostat surface are obtained.

6.2 Fugitive Emissions from Coal Handling

Chapter 2 of Volume I describes the coal handling processes and techniques that are proposed for the hybrid plant (see Figure 2-5, Volume I). This section describes preliminary work that was done to assess the impacts of coal handling on heliostat performance.

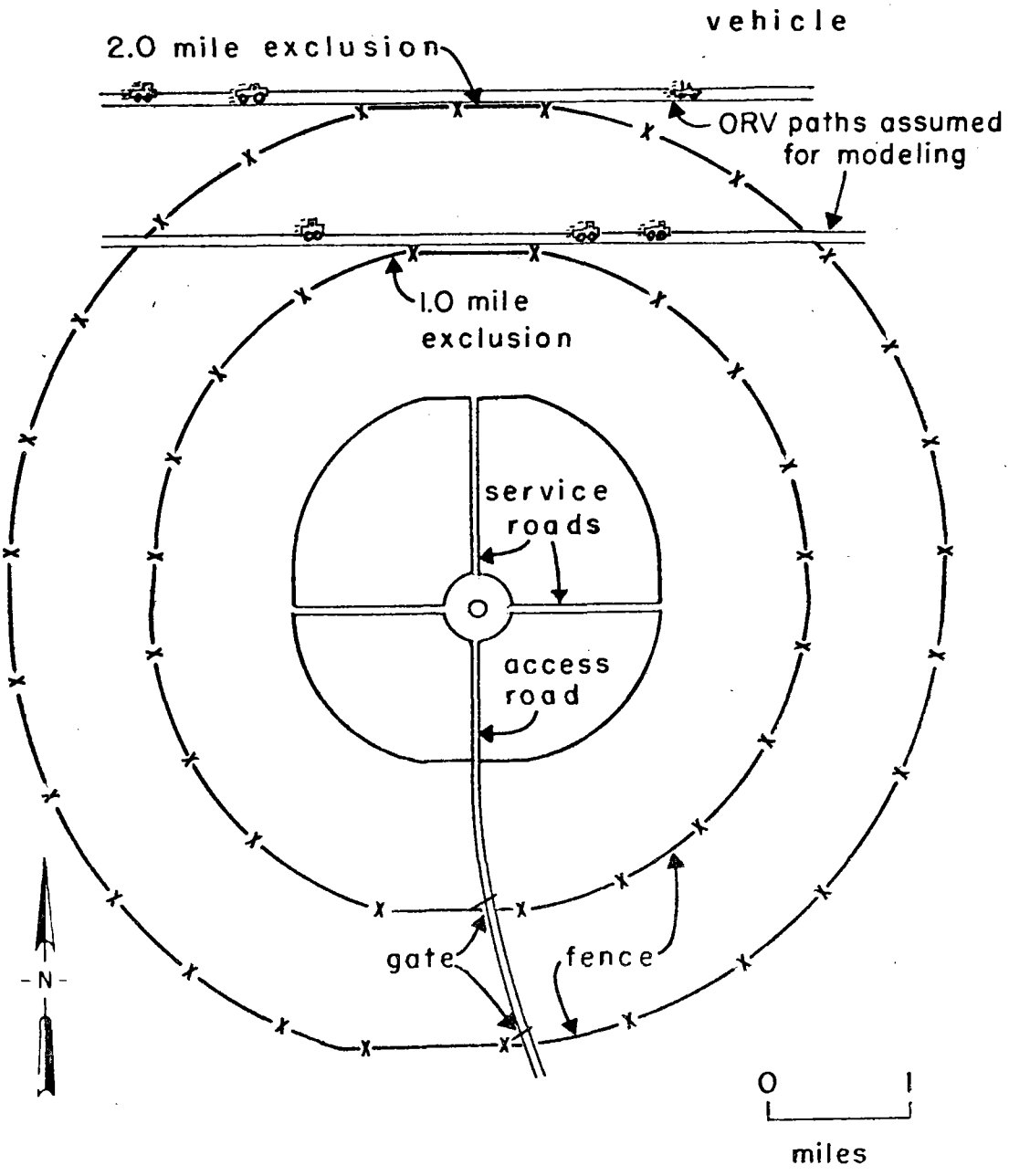

Figure 6-1 Diagram of Scenarios Used in Modeling Fugitive Dust Emissions from the Use of Off Road Vehicles (ORV) Near the Proposed Power Plant

Table 6-1

Estimated Ambient Fugitive Dust Concentrations ($\mu g/m^3$) for a One-Mile Exclusion Zone, Under F Stability

Distance from ORV's	σ_z	$\chi_{24\ hour}$ ($\mu g/m^3$)
2000 m	22 m	34.9
2400	24	32.1
2800	26	29.6
3200	27	28.4
3600	29	26.6
4000	31	24.8
4400	32	24.1
4800	33	23.3
5200	35	22.0
5600	36	21.3
6000	37	20.8

Table 6-2

Estimated Ambient Fugitive Dust Concentrations ($\mu g/m^3$) for a Two-Mile Exclusion Zone, F Stability

Distance from ORV's	σ_z	$\chi_{24\ hour}$ ($\mu g/m^3$)
3600 m	29 m	26.6
4000	31	24.8
4400	32	24.1
4800	33	23.3
5200	35	22.0
5600	36	21.3
6000	37	20.8
6400	38	20.2
6800	39	19.8
7200	41	18.8
7600	42	18.3

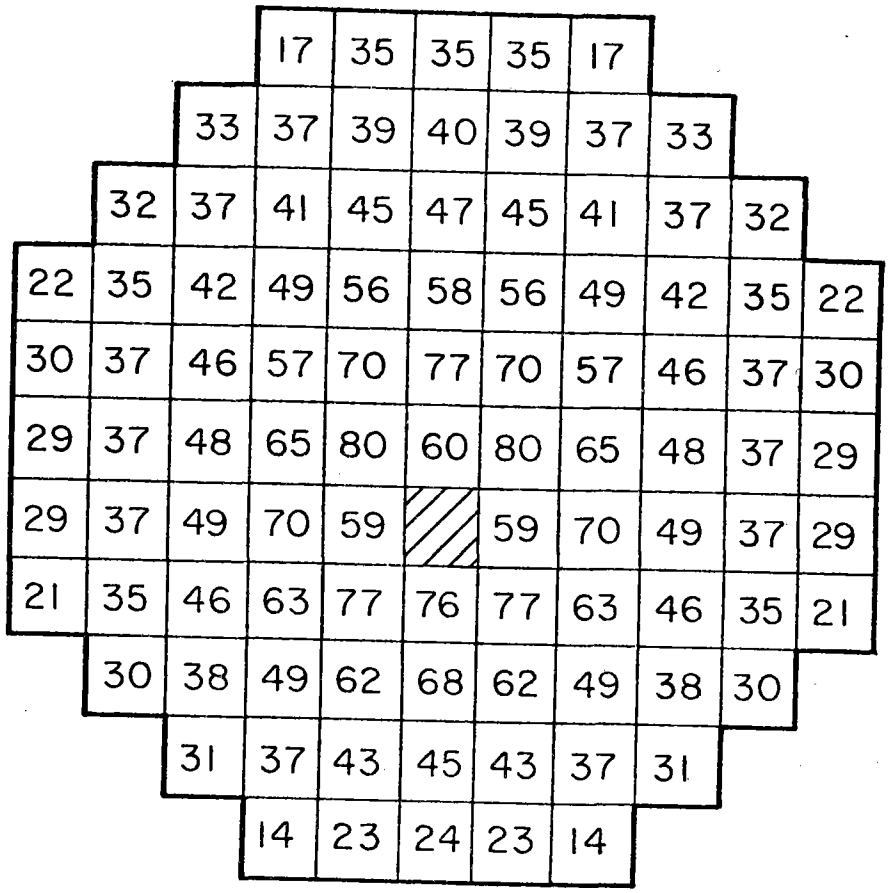

Figure 6-2 Predicted Fugitive Dust Deposition Rates per Cell for a One-Mile Exclusion Zone around the Hybrid Plant (kg/30 days per cell)

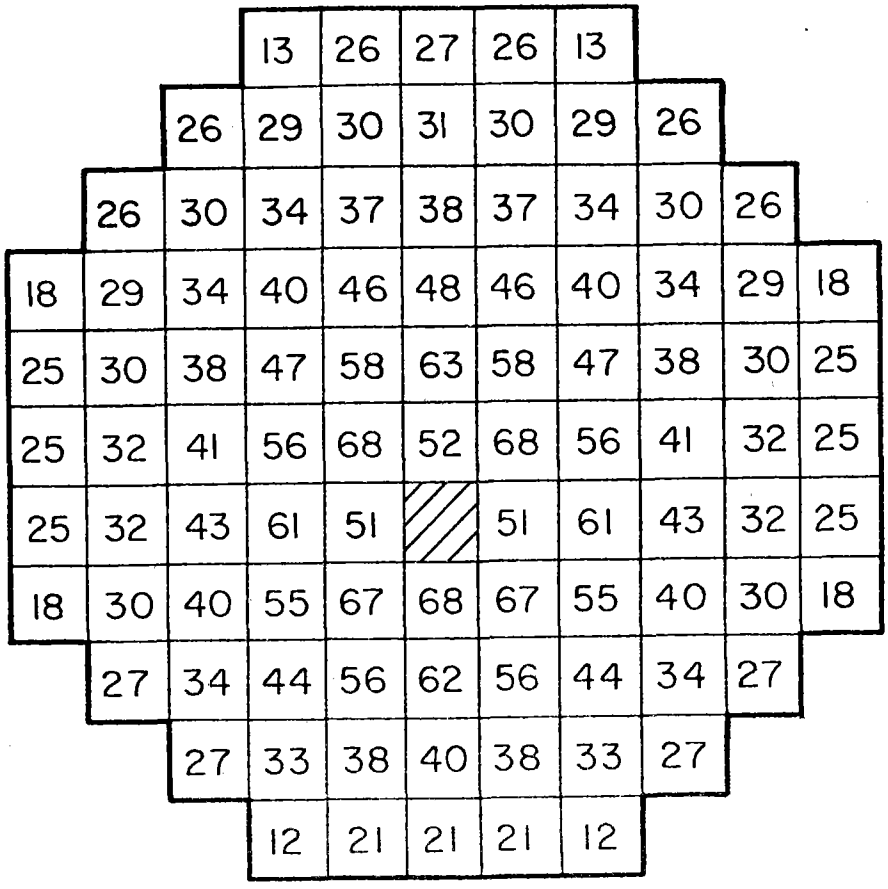

Figure 6-3 Predicted Fugitive Dust Deposition Rates per Cell for a Two-Mile Exclusion Zone Around the Hybrid Plant (kg/30 days per cell)

6.2.1 Worst-Case Emissions

Table 6-3 summarizes the types of coal handling processes, corresponding equations for calculating emission factors, amounts of coal handled, uncontrolled emissions, control techniques resulting from the techniques, and lastly, estimated emissions after application of the control techniques. Emissions were computed by multiplying the emission factor by the quantity of coal handled, and applying control efficiencies where appropriate. Note that emissions for all processes were not computed, pending the receipt of detailed coal handling data from Rockwell. Relevant available coal handling data are summarized in Table 6-3; Volume I describes the data in greater detail.

6.2.2 Worst-Case Meteorology

The various coal sources at the plant are ground and elevated sources, and worst-case meteorology is different for each. For ground level sources (loaders, stockpiles, transfer points) worst-case meteorology is F stability and wind speed of 0.9 m/sec. For elevated sources (hopper building, crusher building, live storage building, and plant coal silos) worst-case meteorology is A stability with 0.9 m/sec wind speed.

6.2.3 Atmospheric Model

Once all the emissions are computed, each process could be modeled as an individual point source using appropriate models (6.12):

$$\text{elevated--}\ \chi(x,y,z) = \frac{Q}{2\pi\sigma_y\sigma_z u}\ \exp\left[-\frac{1}{2}\left(\frac{Z-H}{\sigma_Z}\right)^2\right] + \exp\left[-\frac{1}{2}\left(\frac{Z+H}{\sigma_Z}\right)^2\right]$$

$$\text{ground--}\chi(x,y,z) = \frac{Q}{2\pi\sigma_y\sigma_z u}$$

As an alternative to the above, in order to simplify the modeling without sacrificing accuracy, the following steps could be taken:

- compute an average emission height for groups of sources located near one another;
- if this average height is greater than 100 m, model all these sources as one source with a physical stack height of 100 m;
- if the average height is less than 100 m, then the sources should be modeled as one ground source.

Regardless of which approach is selected, the wind direction should be from the southwest in order to maximize the heliostat area exposed to the emissions.

Once the model is used to predict ambient concentrations, the heliostat particle deposition model could be used to estimate the mass of particles deposited on the heliostat surfaces.

Table 6-3

Summary of Emissions from Coal Handling Processes

Process	Equation/Factor	Quality Coal Handled (tons/yr)	Uncontrolled Emissions	Proposed Control	Percent Reduction	Emissions
Receiving Coal	0.05 lb/T	-		Enclosure/ Collection	95% (6.11)	*
Primary Crushing	0.05 lb/T	-	45 lbs/day	Enclosure/ Collection	95% (6.11)	*
Secondary Crushing	0.15 lb/T	-				
Conveying	0.05 lb/T	-	11 lbs/day	Enclosure (some)	95% (6.11)	*
Transfer Point	0.15 lb/T	-	33 lbs/day	Enclosure/ Collection	95% (6.11)	*
Stockpile Maintenance	$EF = 0.10\ K\ (\frac{s}{1.5})(\frac{d}{235})$ lb/ton $= 0.29$ lb/ton	1953480*	56600 tons/yr	wet dust	50%	28300 tons/yr
Stockpile Wind Erosion	$EF = 0.05(\frac{s}{1.5})(\frac{D}{90})(\frac{d}{235})(\frac{f}{15})$ lb/ton $= 0.095$ lb/ton	1953480*	18,600 tons/yr	wet dust	50%	9300 tons/yr

Source: 6.3 unless otherwise noted. Coal handling data & proposed control obtained from Volume I

* : awaiting further data

* Based on maximum throughput for the dead storage pile, 223 tons/hour boiler feed cate, 365 days/yr.

Table 6-3 (cont'd)

Process	Equation/Factor	Quality Coal Handled (tons/yr)	Uncontrolled Emissions	Proposed Control	Percent Reduction	Emissions
Batch LOAD IN/ LOAD OUT (i.e., where bucket or truck size is known in Yd^3)	$EF = 0.0018 \frac{(\frac{s}{5})(\frac{U}{5})}{(\frac{M}{2})^2 (\frac{Y}{6})}$ $= 8.3 \times 10^{-3}$ lb/ton	-	*	None	-	*

where: s = silt content (coal or road surface) % = 25
S = av. vehicle speed (mph)
W = av. vehicle st. (tons)
d = dry days per year = 345
M = surface moisture content % = 1
U = mean wind speed (mph)
Y = effective loader capacity (yd^3) = 5
K = activity factor = 1
D = duration of storage (days) = 52
f = % of time wind speed exceeds 12 mph = 16.8
e = surface erodibility = 220
PE = Precipiation/Evaporation Index = 4

Some "order-of-magnitude" estimates of the impact of coal handling can be made without computing detailed emissions estimates and performing atmospheric modeling for all the dust sources listed in Table 6-3. Only two of the coal dust sources listed in Table 6-3, stockpile maintenance and stockpile wind erosion, are likely to produce appreciable quantities of dust. The other dust sources are either effectively controlled, or are not significant due to the relatively small quantities of coal that are proposed to be handled at the plant. Fugitive emissions from the dead coal stockpile were computed using the worst-case assumption that the coal plant is using coal at the maximum burn rate (223 tons/hour, 24 hours/day, 365 days per year). It was also assumed that all coal passes through the dead coal pile. Fugitive emissions from stockpiles tend to be greatest when coal is being added to and removed from the stockpile. Assuming that all coal passes through the dead pile is therefore another worst-case assumption.

The dead coal stockpile is expected to emit 37,600 tons/yr of dust as a worst-case, through maintenance and wind erosion combined. This figure translates into a worst-case mass emission rate of approximately 1100 grams/sec. Assuming that the stockpile is 30 m tall, under Class F atmospheric stability the emissions will reach a maximum ($\chi\mu/Q$) value of 1×10^{-4} m^{-2} at a downwind distance of approximately 1500 m (6.12). This location is within the heliostat field if the wind blows from the west, as shown in Figure 2-2. Assuming a wind speed of 1 m/sec, the maximum ambient concentration would be approximately 1.1 g/m^3. This figure is considerably larger than the ambient particulate levels predicted to result from coal combustion and would result in large particle impaction rates on heliostat surfaces. However, it is based on unrealistic worst-case assumptions and should thus be treated with caution. Nevertheless, the exercise does show that fugitive emissions from coal handling could be a serious problem at the facility.

6.3 Vehicle Operation Within the Plant

Recognizing that vehicle operation within the plant boundaries will produce fugitive dust, Rockwell proposed to pave all the access and service roads and so minimize fugitive dust emissions. Nevertheless, some fugitive dust is generated by vehicle traffic even on paved roads, through re-entrainment. Tire wear and vehicle exhaust also contribute particulate matter, but these are non-fugitive sources. Average emissions of entrained dust on paved roads is approximately 3.2 g/km-vehicle, excluding exhaust and tire wear (which contribute about an additional 0.3 g/km-vehicle). The factor is not corrected for wet days because mud will be deposited on the roads during wet periods, and when drying, the mud will contribute to dust re-entrainment levels (6.13).

The emissions from vehicle activity on access and service roads can be calculated using the model described in Section 6.1. Detailed data on the number of vehicles expected to be operating on the roads of the facility are needed to accurately estimate ambient dust levels resulting from vehicle operation. The length of the roads can be obtained from Figure

2-2 and Volume I. For the east-west roads, the worst-case wind direction should be assumed to be southerly; for north-south roads, the worst-case wind direction should be assumed to be easterly or westerly. The simplified model assumes that the wind is perpendicular to the road. Other models exist which treat wind direction at acute angles to the line source being studied (6.9).

6.4 Fugitive Dust Impacts on the Environment

The construction of the proposed facility in a desert environment will likely have adverse impacts on the surrounding environment because it will result in considerable fugitive dust emissions. Two major types of activities will affect fugitive dust emissions:

- clearing the land of natural vegetation so construction can begin; including grading and excavation.
- construction of the facility.

As indicated in Volume I, the proposed plant will require about 3000 acres, not including the exclusion zone. An exposed area of that size in the desert is expected to lose approximately 4 million tons of dust per year, as calculated from the following equation (6.3):

$$EF = 3400 \frac{(\frac{e}{50})(\frac{s}{15})(\frac{f}{25})}{(\frac{PE}{50})^2} \text{ lbs/Acre/Yr}$$

where:

e = surface erodiability = 220 for sand (6.3)

s = silt content = 25% for dirt roads (6.3)

f = % of time wind speed exceeds 12 mph (6.14)

PE = precipitation/evaporation index = 4 (6.3)

This large amount of material would undoubtedly be deposited mostly on the northeastern side of the site, because the prevailing low-level wind is from the southwest, as shown in Figure 6-4 (6.15). Similar effects have been observed during the construction of the Barstow Solar Plant site; a "corona" of sand formed from wind erosion of the exposed area, as can be seen by inspection of aerial photographs of the site (6.16). The reason for concern is not that the material is "lost" from the site, but rather that if material was light enough to be blown away in the first place, it could easily blow back onto the site (and heliostats) when gusts of wind not in the direction of the prevailing wind occur at the site. Hence unless the corona is covered or sprayed to prevent wind erosion, it represents a potential area source of pollution that could contribute to heliostat degradation. Also, the eroded dust could have adverse impacts on the ecology surrounding the site.

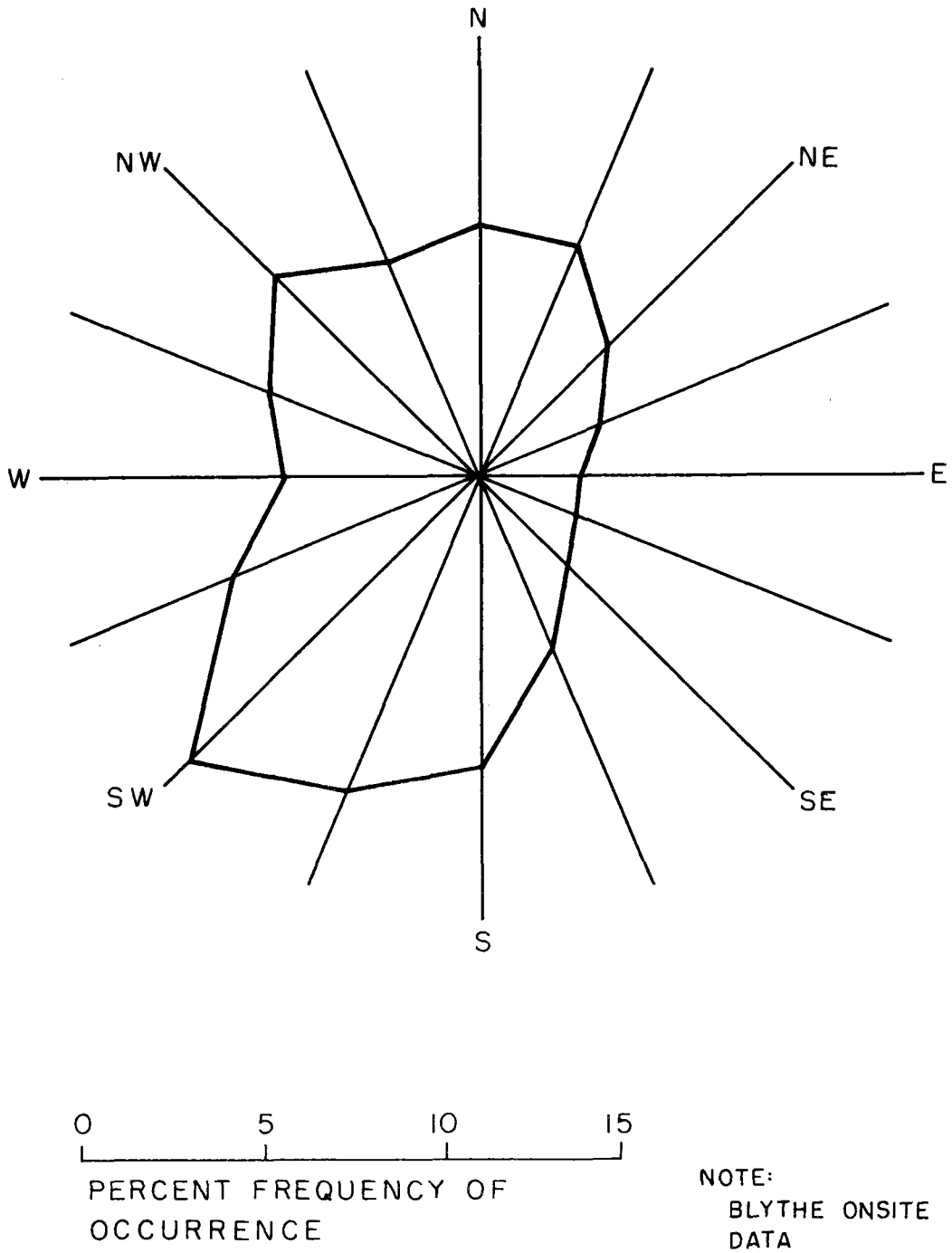

Figure 6-4 Wind Distribution Rose 33 ft. Observations
Period: 6/1/75 - 5/31/76 (Reference 6.15)

Once the site is cleared, construction activity itself can be a further source of fugitive dust. Construction activity is estimated to produce 1.2 tons of fugitive dust per acre of construction per month (6.17). Assuming that the 3000 acre plant will take 60 months to construct, approximately 216,000 tons of dust will be removed from the site over the five-year period, with the same potential adverse impacts as those discussed above.

Fine soil material is abundant in the desert, but it is formed at the surface into a thin crust which protects the underlying fines from erosion. The crust may be up to 6 mm (0.2 inches) thick. Disturbance of the "desert crust" by construction operations would result in a fugitive dust increase and degradation of soil quality due to erosion. "Desert pavement" is formed by densely packed pebbles and stones. These stones are cemented together or encrusted with various salts, gypsum, lime, and silicates, and are often coated with a "desert varnish." The pavement retards erosion and surface water runoff. The breaking of desert pavement by construction would result in increased fugitive dust emissions and water erosion of soils. Rainwater penetration or recharge to groundwater would be decreased (6.18).

6.5 Phytogenic Emissions

This section estimates the rates at which gaseous hydrocarbons are emitted from natural desert vegetation. Only gases will be addressed here, although some desert plants also "emit" particulates in the form of salt particles; little data is available on these particulate emission rates, so they will not be addressed. The primary concern here is whether or not sufficient amounts of natural organics will be emitted by vegetation, and will travel to the heliostats and condense on the cool heliostat surface, to possibly degrade reflectivity themselves, or, more likely, to serve as collectors of fine dust particles that could affect reflectivity.

The most prevalent vegetation type around the site is larrea (creosote bush) (6.19). Very little information on hydrocarbon emission rates for this plant exist in the literature. However, it is highly resinous and emissions would be seasonal. It was assumed that the creosote bush would most likely resemble conifers in terms of emission rates. Table 6-4 summarizes the data that have been collected for vegetation types, on the biome level in desert environments (6.20). Therefore, the worst-case emission rate selected for larrea would be 222 g/m^2-hour.

A rough inspection of the vegetation distribution map (Volume I, Figure 3-5) indicates that about 4 mi^2 area of creosote exists to the south of the site. Four square miles results in a worst-case emission factor of 0.63 g/s. The ambient levels resulting from these emissions could be estimated by treating the creosote as a ground level area source. As a worst-case, one could then assume that most or all of the vapors would condense on the heliostat surface, according to the heliostat particle impaction model.

Table 6-4

Desert Biome Emission Factors
(Standarized to 30°C)

	Leaf Biomass Density (g/m^2)	Emission Rate (ER)		
		Day $\mu g/m^2$ hr	Night $\mu g/m^2$ hr	Winter $\mu g/m^2$ hr
Conifer	25	222.5	222.5	88
Oaks	25	617.5	117.5	0
NC-NI	40	172.0	172	0
NC-I	10	103.0	24	0
LL	--	162	162	0
	100	1277	698	88

KEY:

NC-NI = non-conifer, non isoprene emitting species

NC-I = non-conifer, isoprene emitting species

LL = leaf litter

(Source: Reference 6.20)

In addition to the vegetation near the proposed site, phytogenic emissions from large areas of vegetation located upwind could be significant. Furthermore, insects could also be a problem in terms of heliostat fouling, as could bird droppings.

6.6 Natural Dust Emissions

Sections 6.1 through 6.5 dealt with a worst-case analysis of the impacts of man's activities on heliostats, in terms of fugitive dust emissions. Natural dust "emissions" could also have a significant worst-case impact on the heliostats. The occurrence of sandstorms and dust storms at the site will not only force the shut down of the solar component, but probably will also deposit significant amounts of sand and dust on the heliostats. Most likely the plant operator will receive advance warning of such storms, and will stow all the mirrors in the face down position before arrival of the storm. However, as discussed previously, even mirrors stowed face down collect fine particulates on their surfaces. Table 6-5 present the frequency of occurrence of dust storms and sandstorms at the site. The impacts of these phenomena can't be quantified with models, etc., to the extent that was done for impacts of other particulate generating processes. From a qualitative standpoint, these storms will most certainly result in the deposition of sufficient amounts of fine particulates on the heliostat surfaces to require heliostat cleaning before the solar component can be operated at full capacity.

6.7 Summary

Preliminary estimates of fugitive particulate emissions and resulting ambient concentrations indicate that the impacts of these emissions can be comparable in magnitude to impacts from non-fugitive emissions. Further studies should be done to refine the estimates given in this Section. Fugitive emission estimates, because of their nature, are even less accurate than their counterparts. Uncertainties in fugitive emission factors can range from a factor of two to an order of magnitude (6.22). This uncertainty is compounded by the dispersion model, which is accurate to approximately a minimum of a factor of five (6.23). If refined estimates indicate that fugitive dust can have a significant impact on solar operation, then the potential utility of solar power through large-scale solar plants sited in the desert is made less certain, because mitigating the fugitive dust impacts may prove to be very difficult. Mitigation measures such as enclosing the solar plant with an air foil that would inhibit fugitive dust from entering the plant site perhaps deserve further study.

Table 6-5

Distribution of Occurrence of
Blowing Sand or Blowing Dust Storms
at Blythe, California, Relative to
Wind Speed and Visibility

Wind Speed (mph)	Number of Occurrences	Visibility (miles)	Number of Occurrences
6-10	2	0 - 0.25	4
11-15	10	0.26 - 0.50	9
16-20	34	0.51 - 0.75	1
21-25	28	0.76 - 1.00	12
26-30	23	1.01 - 1.50	3
31-35	17	1.51 - 2.00	5
36-40	5	2.01 - 3.00	24
41-45	3	3.01 - 5.00	51
>45	0	$\geq$5.00	13

6.8 References

6.1 U.S. Environmental Protection Agency, "Compilation of Air Pollutant Emissions Factors." Third Edition, Supplement Number 8. Office of Air and Waste Mangement, Office of Air Quality Planning and Standards, Research Triangle Park, North Carolina, p. 11.2.1-1 (May 1978).

6.2 King, D.L. and J.E. Meyers. "Environmental Reflectance Degradation of CRTF Heliostats." Sandia Laboratories, Division 4713, Albuquerque, New Mexico (1978).

6.3 State of Colorado, Air Pollution Control Division. "Emission Factors for Mining Operations." Two-page worksheet, Denver, Colorado (March 1978).

6.4 Reference 6.3, page 2.

6.5 The vehicle weight of 1 ton was arbitrarily chosen, but it is thought to be a reasonable average ORV weight. Many types of ORV's are used in the desert, ranging from lightweight trail motorcycles and mini-bikes to heavier four-wheel drive pick-up trucks and jeeps.

6.6 Reference 6.1, page 11.2.1-3.

6.7 Reference 4.11, page 38.

6.8 San Diego Gas & Electric Company, "Environmental Report, Construction Permit Stage, Sundesert Nuclear Plant, Units 1 and 2." Volume 2, Figure 2.3-9 (June 1977).

6.9 Turner, D.B. "Workbook of Atmospheric Dispersion Estimates." U.S. Department of Health, Education and Welfare, PHSP, No. 999-AP-26, p. 40 (1969).

6.10 Reference 6.1, p. 11.2.1-4.

6.11 PEDCO-Environmental Specialists, Inc. "Evaluation of Fugitive Dust Emissions from Mining, Task 2 Report, Assessment of the Current Status of the Environmental Aspects of Fugitive Dust Sources Associated with Mining." Prepared for U.S. EPA under Contract No. 68-02-1321, Task #36, Cincinnati, Ohio (June 1976).

6.12 Reference 6.9, p. 29.

6.13 Reference 6.1, Supplement Number 9, p. 11.2.5-3 (July 1979).

6.14 Reference 6.8, Table 2.3-10; computed by summing the wind speed frequency distribution data in the table for all wind speed classes over 12 mph.

6.15 Reference 6.8, Figure 2.3-5.

6.16 Lindberg, R.G. Environmental Effects of Solar Thermal Power Systems: Quarterly Report of Progress. (UCLA 12-1187-11). Laboratory of Nuclear Medicine and Radiation Biology, UCLA (June 1980).

6.17 Reference 6.1, Supplement Number 7, (August 1977).

6.18 Davidson, M., D. Grether, and K. Wilcox. Ecological Considerations of the Solar Alternative. Lawrence Berkeley Laboratory, Berkeley, California, p. 13 and 15, LBL-5927 (1977).

6.19 Reference 6.8, Early Site Review, Volume 4, Figure Number 2.2-2, Vegetation Cover Types, (April 1976).

6.20 Zimmerman, P.R. "Testing of Hydrocarbon Emissions from Vegetation, Leaf Litter and Aquatic Surfaces, and Development of a Methodology for Compiling Biogenic Emissions Inventories." Final Report Prepared for the U.S. Environmental Protection Agency, Office of Air Quality Planning and Standards, EPA-450/4-79-004 (March 1979).

6.21 Reference 6.8, Table 2.3-7, Volume 2.

6.22 Budiansky, S. "Wanted: Fugitive Emissions." Summary of Session on Non-point Sources of Air Pollution held at the Annual Meeting of the Air Pollution Control Association, Environmental Sci. Technol. 14: 904-905 (1980).

6.23 Turner, D.B., "Atmospheric Dispersion Modeling, A Critical Review." J. Air Poll. Control Assoc., 29: 502 (1979).

7.0 WEATHER MODIFICATION

Discussion, conjecture, and some modeling of possible weather modification from large heat sources have appeared in the literature. Included are power plants and cooling towers in general and large scale solar thermal conversion facilities. The literature documents many accounts of the influences of local heat islands (cities and industrial parks) in modifying weather or generating clouds (7.1). This section discusses the effects of power plants in general (cooling towers), and also solar power plants on local (site and adjacent land uses) and regional concerns (thousands of kilometers).

7.1 Power Plants and Cooling Towers

An assessment of the potential meteorological impact of heat from power plants can be made by comparing their thermal energy with the energy content of naturally occurring phenomena (see Table 7-1). Power parks (complexes of 5-20 power plant units) and cities release heat at rates comparable to the energy content of several natural phenomena, so one would expect power parks and cities to possibly influence weather. The total energy release from a single cooling tower is much smaller than any of the natural events except the tornado. If energy fluxes are compared, the single cooling tower appears to be able to influence atmospheric conditions, but only on a small scale--a small, intense thermal which could produce a cloud or "dust devil" (whirlwind). Studies indicate that a single cooling tower has too much buoyancy relative to its size to permit the development of vorticity needed to produce a tornado. Recorded cases of altered precipitation related to power plant operation do exist (7.3).

The amount of energy released as heat to the condenser of steam-electric plants can exceed twice the amount of electrical energy generated. A dry-cooling system increases fuel usage and therefore heat dissipation because of lower plant thermal efficiency. Speculation indicates the heated plume from dry-cooling towers could result in cloud formation, modification of precipitation patterns, fog dispersal, local heating, and air exchange in a stagnant air basin. Kearney and Boyack (7.4) discusses plume behavior and potential environmental effects of dry cooling towers for a 1,000 MWe power plant.

In unstable atmospheric situations, plumes from large dry-cooling towers can rise to 300 meters (10,000 feet) and occasionally produce a visible cloud. Plumes are not likely to produce large clouds or clouds which develop substantial precipitation even with the most favorable meteorological conditions. The horizontal velocity of air movement 20 meters (70 feet) from the tower would be less than eight kilometers per hour (five miles per hour). Air movements would not be detectable at ground level for distances greater than 150 meters (500 feet) from the tower. Transport of air pollutants by the thermal plume's penetration into the inversion layer would be marginal. A 3° F air temperature rise could occur within a 1.6-kilometer (1-mile) radius of the tower; while a 0.1° F temperature rise could occur within an 8-kilometer (5-mile) radius of the

Table 7-1

Approximate Energy Production Rates of Some Natural and Anthropogenic Sources

	Energy Flux W/m^2	Total Energy MW
Solar energy flux on ground (global average)	100	
Cyclone	200	10^8
Thunderstorm (1 cm of rain in 30 min.)	1000	10^5
Tornado (lasting for 10 min., covering 1000 sq. meters)	10^5	100
Volcanic heat output (Surtsey)	10^5	10^5
Bush fire	2000	10^5
City of New York	650	$4x10^4$
City of St. Louis	650	$1.6x10^4$
20 GWe power park (33% efficient, covering 10 km^2)	4000	$4x10^4$
20 GWe power park (33% efficient, covering 100 km^2)	400	$4x10^4$
500 MWe single cooling tower (10 m diameter)	10^5	10^3

Reference 7.2

tower. (This assumes the tower heat discharge is completely mixed with a volume of the surrounding air.) A more likely meteorological condition which would increase local air temperature is the forcing of the plume to the ground at some distance from the tower (fumigation). This could result in a maximum temperature rise at ground level of 20° F. Warm, dry air from the tower has the potential for dispersing fog, but it will probably pass quickly through a fog layer. Ingress of air into the tower might prevent fog formation near the ground within a radius of 150-300 meters (500-1,000 feet) (7.4). It is concluded that dry cooling tower heat discharges for a 430 MWe power plant would not significantly modify local meteorological conditions.

There exists a general understanding of many aspects of cooling tower plume behavior, but the understanding is neither complete nor quantitive enough to predict in detail certain critical characteristics of plumes. Typical heights and lengths of visible plumes can be estimated with tolerable accuracy, and the relationship of these variables to mean properties of the atmosphere are generally understood (7.5). This same source concluded, "with regard to drift deposition, ground fog, and weather effects we have inadequate data and analytical capability for detailed prediction. No capability for modeling ground fog and weather effects with any accuracy has been demonstrated."

To modify weather artificial heat sources must have energy comparable to natural atmospheric phenomena, and this energy must be organized (i.e., thermal energy must be converted into appropriate motional forms). Analyzing such a transformation requires an understanding of the development of convective systems that is currently lacking. Further complicating the situation is the possibility that heat release could stimulate natural phenomena by triggering latent instabilities. This process is not well understood either (7.3). Atmospheric heat rejection by power plants is being studied through the METER program (Meteorological Effects of Thermal Energy Release) sponsored by the Department of Energy. This program is aimed at a long-term assessment of the problem, starting with an emphasis on understanding the effects of existing power plants.

7.2 Solar Power Plant--Central Tower Configuration

A solar thermal power plant has the potential for affecting local and regional climate through the following mechanisms:

- Changes in the surface-energy balance, resulting from changes in the reflectivity (albedo) of the surface or its thermal characteristics.
- Changes in surface roughness caused by power plant ancillaries and installation of heliostats.
- Changes in surface moisture.

- Dissipation of waste heat into the atmosphere from cooling systems.

Figure 7-1 shows the distribution of solar energy at the earth's surface before and after installation of a solar power plant.

7.2.1 Regional Effects

One must be able to compare a solar power plant's impulses with already existing thermal, stress, and moisture anomalies. Soil and rock type, vegetative cover, soil moisture, antecedent precipitation patterns, surface roughness, and other factors combine with changes in stability and low-level wind structure to give rise to complex patterns of convergence, divergence, and convection. Natural influences are as great or greater than the localized heat source of a power plant (see Table 7-1). In most situations existing disturbances will set the pattern of convection, and man's influence would be lost within the natural pattern. If, however, the wind tends to be from the same direction during periods when impulses of the magnitude of those induced by man can have an effect, it is reasonable to expect a precipitation anomaly downwind (7.1). A power plant's influence on weather is site specific; where land forms, land use and character are varied, the influence of man-made heat sources may be hard to determine.

Meteorological impacts from a 30 GWe solar thermal power plant (central tower) in southern Spain have been modeled. The heliostats for such a plant would cover eight square kilometers; the heliostat area for the proposed coal/solar hybrid power plant for this study would cover just one eighth as much (on square kilometer). Figure 7-2 shows land surface temperatures before and after installation. The surface temperature immediately above the heliostat field was significantly lower than surrounding surface temperatures. The temperature difference for before and after the heliostat field construction was approximately 4 to 8° C. The power plant caused the model atmosphere to be relatively more moist than the control case and clouds formed. The high reflectivity of the heliostats captured the solar radiation that would otherwise be absorbed by the ground surface. This resulted in a decrease in convective (buoyant) activity over the mirror-covered area. This modeling represents a "worst-case situation" because the heliostats were assumed to be packed close together rather than spaced throughout an area four times larger than their surface (32 square kilometers). The results of the modeling study suggest the possibility of more pronounced and persistent formation of clouds and rain if a large-scale solar thermal power plant is installed in an area with summer meteorological conditions such as those assumed for southern Spain. These effects would extend to a distance of a few hundred kilometers from the power plant (7.8).

Potter and MacCracken (7.9) even attempted to model global effects from a large scale solar plant.

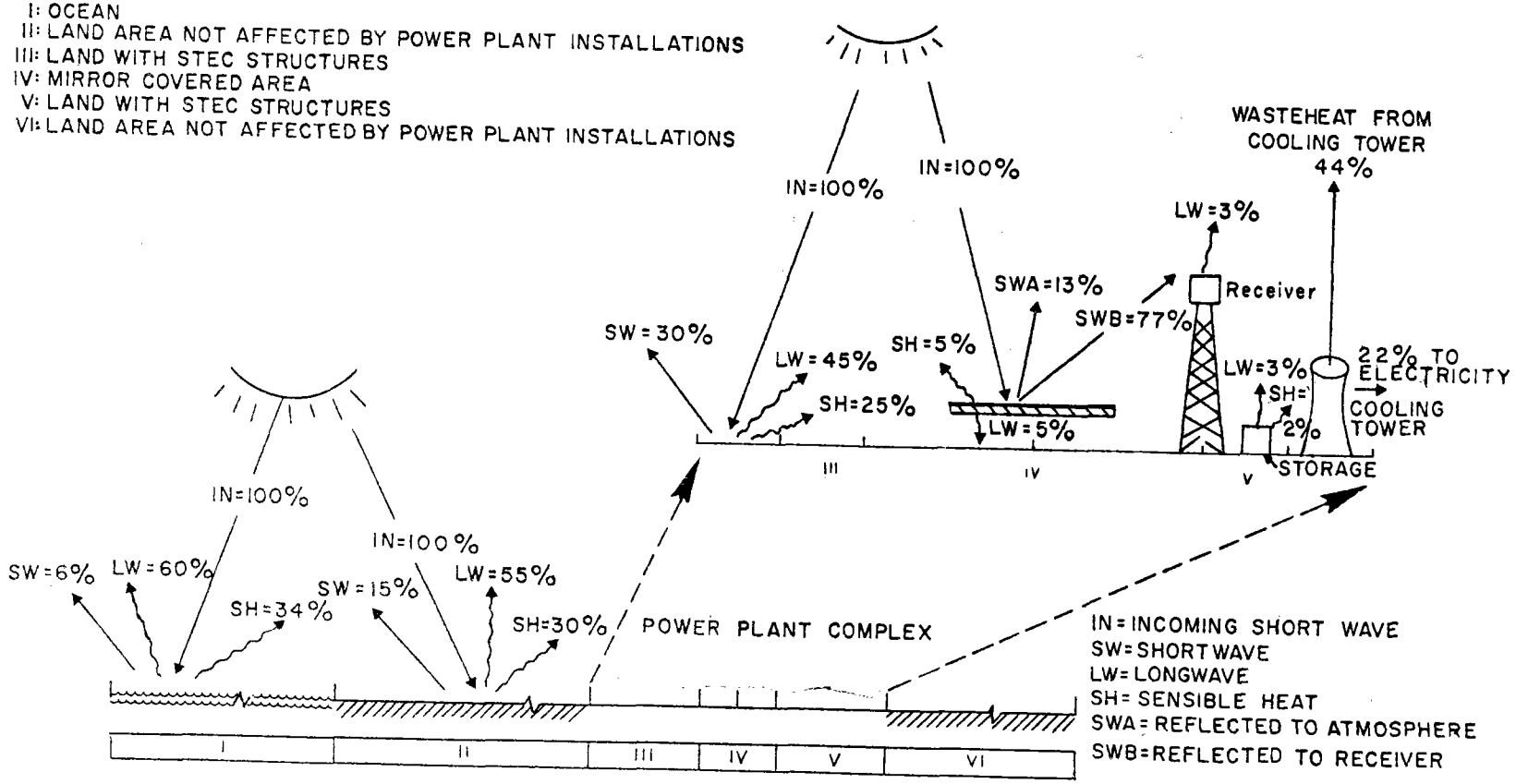

Figure 7-1 Distribution of Solar Energy at the Earth's Surface Before and After Installation of a Solar Power Plant

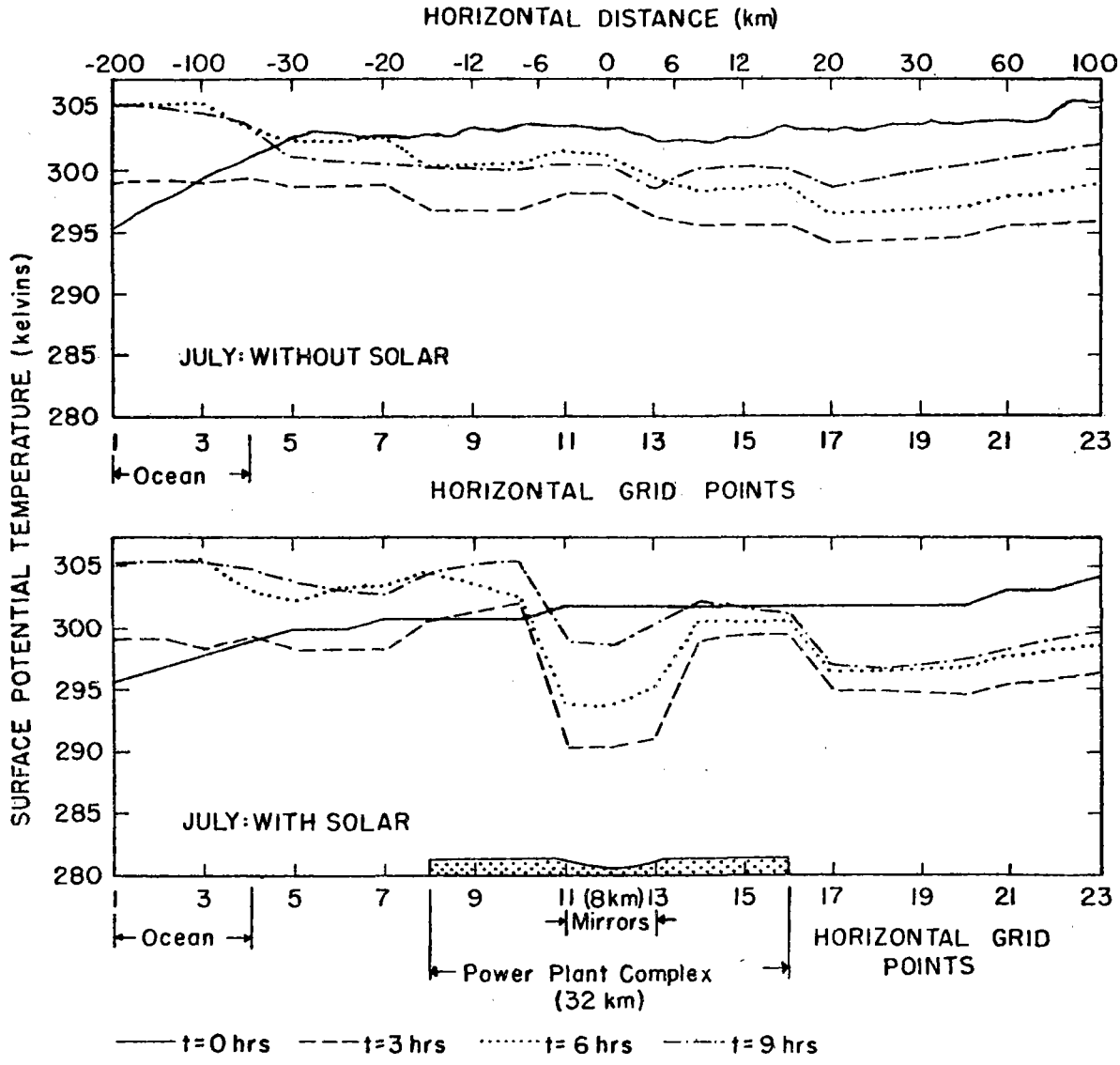

Figure 7-2 Surface Potential Temperature at T = 0, 3, 6 and 9 Hours in Summer Before and After Solar Power Plant Installation T = 0 is 0800 Local Time (Spain) (Reference 7.7)

7.2.2 Local Effects

Much speculation and a few measurements provide information regarding the effect of heliostats on atmospheric and soil moisture conditions within a heliostat field. Such localized or site-specific effects are important for evaluating the possible plant and animal species changes that might take place due to siting a solar power plant.

Heliostats would shade the ground underneath them. A 25 percent ground coverage by heliostats would probably result in a 50 percent decrease in total incident radiation to the ground surface. Radiant temperature (temperature that a black body would have to be at to produce thermal radiation equal to the downward counterradiation of the sky), surface temperature, and soil temperature are expected to be reduced under the heliostat field; these predictions are based on temperatures measured under desert vegetation. Ambient air temperatures would probably not be significantly reduced. Soil moisture under the heliostat field would probably be greater than for open desert, especially if heliostat wash water is allowed to fall on the ground (7.10).

Heliostats would disturb low-level air flow patterns. Patten (7.10) feels that wind deflection would probably not affect air temperatures, whereas another source states that wind speeds below the heliostat surfaces would decrease and possibly reduce air and surface temperatures (7.11). Light wind speeds and cooler temperatures beneath the heliostats would probably reduce evapotranspiration within the field significantly (7.10, 7.11). Reduced air and ground surface temperatures, reduced evapotranspiration, and shading of the ground beneath the heliostats may create the microclimate conditions of a north-facing slope inside the heliostat field.

Some measurements have been taken under heliostats (see Tables 7-2 and 7-3 and Figure 7-3) and some results appear contradictory to impacts hypothesized. Air movement at 20 cm (8 inches) was reduced within the mirror array by 34-86 percent. Reduced air movement appears to become more significant as total air movement decreased. Air temperatures measured under the heliostat array at heights of 10, 30, and 100 cm (4, 12, and 39 inches) were higher than in the open desert. This may be caused by reduced long-wave radiation loss and air movement. Soil temperatures in the shaded gaps between heliostats were lower than soil temperatures immediately under heliostats (7.10).

7.3 Conclusions

Large energy centers are likely to influence the location and perhaps the magnitude of convective shower and storm systems. They may also initiate new convective activity, such as thunderstorms and even tornadoes; however, this is most likely to occur when natural disturbances are already present. Large energy centers could impact regional climate (thousands of kilometers). Small heat sources such as individual cooling towers would affect only the site area. Although quantitative predictions of meteorological effects from power plant operations cannot be made,

Table 7-2

Air Movement Within the Solar Collector Field Compared to Air Movement in the Control Open Desert at 25 cm Above the Ground Surface

Dates (1977-78)	Site	Total Mileage	Miles Per Day
Dec. 16-20	Array	78.1	19.5
	Open Desert	117.9	29.5
Dec. 20-30	Array	73.3	7.3
	Open Desert	147.4	14.7
Dec. 30 - Jan. 3	Array	7.8	1.95
	Open Desert	56.0	14.0

Reference 7.10

Table 7-3

Averages of Maximum and Minimum Air Temperatures Taken Periodically at Three Different Heights Above the Ground Within the Collector Simulator Array and in the Open

Height	Site	Average Maximum (°C)	Average Minimum (°C)
100 cm	Array	24.6	3.3
	Open Desert	21.5	5.3
30 cm	Array	24.0	3.05
	Open Desert	22.4	3.05
10 cm	Array	23.5	4.6
	Open Desert	20.0	3.5

Reference 7.10

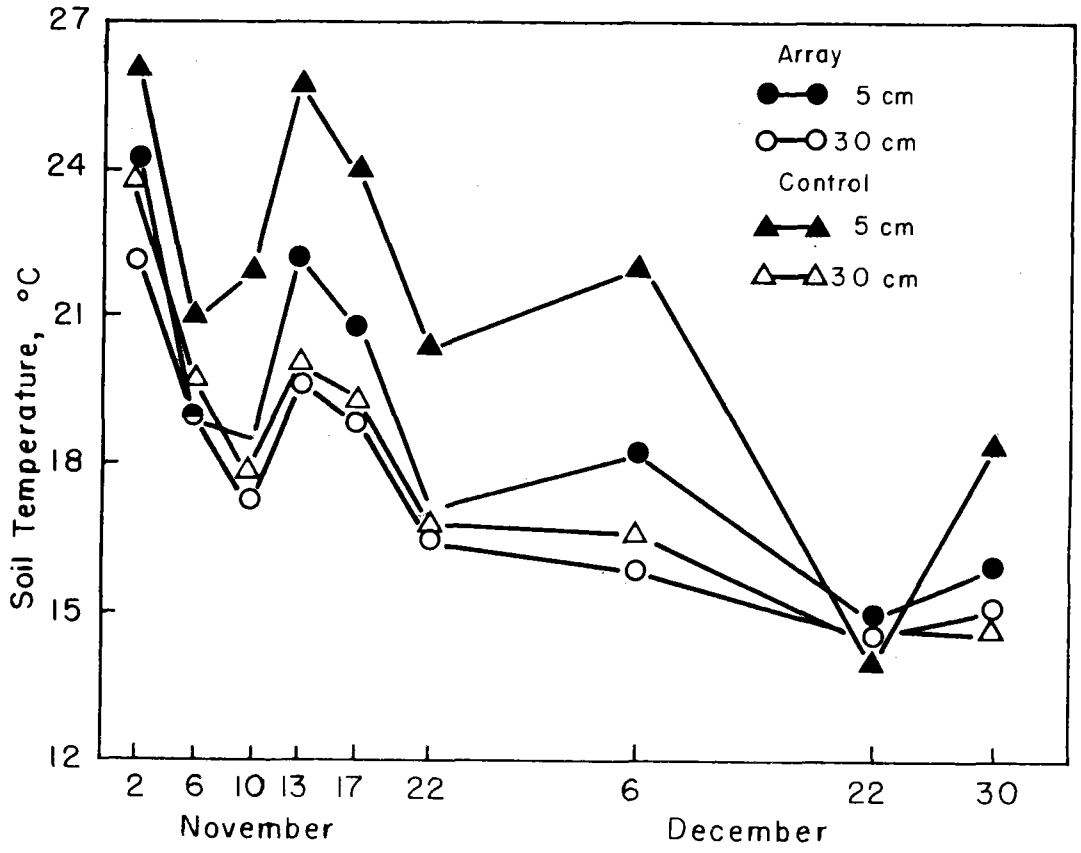

Figure 7-3 Average Soil Temperatures at 5 cm and 30 cm Depths Within the Solar Collector Arrays and Without Control Site (Reference 7.10)

evidence indicates that existing plants (up to 4000 MWe) rarely produce noticeable weather changes, although they may cause cloud formation (7.1).

Climate changes from a 430 MWe coal/solar hybrid power plant would not be significant on a regional scale. With correct atmospheric conditions, the heat from this plant could induce cloud formation with resulting precipitation downwind of the site. Cloud formation would reduce solar insolation and affect the efficiency of the solar portion of the plant (intra-plant impact). Precipitation falling on the heliostat field, if sufficient, could clean the mirror surfaces and result in a saving of wash water. Climate modifications within the heliostat field would result in a cooler and moister habitat and probably result in a change in species type and diversity as compared to the surrounding desert. Actual climate modifications from a solar power plant will not be predictable until a test facility such as the Barstow plant is built and operating.

7.4 References

7.1 Hosler, C.L. and H.E. Landsberg. "The Effect of Localized Man-Made Heat and Moisture Sources in Mesoscale Weather Modification." In National Academy of Sciences, Energy and Climate, Studies in Geophysics, Washington, D.C., 96-105, p. 98 (1977).

7.2 Laurmann, J. Modification of Local Weather by Power Plant Operation, Electric Power Research Institute, Palo Alto, California, p. 4 (1978),

7.3 Reference 7.2, pp. 3, 4, and 5.

7.4 Kearney, D.W. and B.E. Boyack. "Plume Behavior and Potential Environmental Effects of Large Dry Cooling Towers." In R.L. Webb and R.E. Barry, eds. Dry and Wet/Dry Cooling Towers for Power Plants, The American Society of Mechanical Engineers, New York, 35-48 (1973).

7.5 Research Committee on Atmospheric Emissions and Plume Behavior from Cooling Towers, American Society of Mechanical Engineers. Cooling Tower Plume Modeling and Drift Measurement A Review of the State-of-the-Art, New York (1975), pp. 59 and 118.

7.6 Bhumralkar, C.M., J. Williams, and A. Slemmons. "The Impact of a Conceptual Solar Thermal Electric Conversion Plant on Regional Meteorological Conditions: A Numerical Study." Solar Energy 23:393-403 (1979), p. 397.

7.7 Reference 7.6, p. 399.

7.8 Reference 7.6, pp. 393-403.

7.9 Potter, G.L. and M.C. MacCracken. Possible Climatic Impact of Large Scale Solar Thermal Energy Production. Lawrence Livermore Labs., Livermore, California, UCRL-78855 (1977), 16 pp.

7.10 Patten, D.C. Solar Energy Conversion: An Analysis of Impacts on Desert Ecosystems, Final Report. Arizona State University, Tempe, COO-4339-3 (1978), 100 pp.

7.11 Department of Energy. Environmental Development Plan (EDP), Solar Thermal Power Systems. Washington, D.C., DOE/EDP-0004 (1978), p. 20.

8.0 CONCLUSIONS AND RECOMMENDATIONS

8.1 Intra-Plant Air Quality and Meteorology

The purpose of this report has been to identify air quality and meteorology issues that need to be studied in detail in order to properly assess the environmental impacts of a 430 MWe coal/solar hybrid power plant. The work described in the previous chapters has been essentially a screening exercise.

Based on the results of this study, the following issues should be treated in more detail and with greater technical sophistication in order to assess the air quality impacts of the coal/solar hybrid plant:

- particulate emissions from coal combustion depositing on heliostat surfaces;
- salt particle emissions from cooling tower operation depositing on heliostat surfaces;
- attenuation of insolation by coal combustion and cooling tower plumes;
- particle emissions from off-site activities depositing on heliostat surfaces;
- particle emissions from coal handling depositing on heliostat surfaces.

The preliminary work done in this volume indicates that, as a worst case, in a 30-day period, several hundred grams of particulate matter from coal combustion might deposit on a single heliostat surface. Salt particle deposition from cooling tower operation and off-site fugutive dust could add comparable amounts under their respective worst-case scenarios. Natural emissions and fugitive emissions from coal handling could also deposit significant but as yet unquantified amounts of matter on heliostat surfaces. Thus, a worst-case estimate would be that as much as kilogram quantities of matter could be deposited per heliostat in a 30-day period.

Based on information in the current literature, the plant is not expected to significantly affect climate on local or regional scales.

The ramifications of these preliminary results are twofold:

- The proposed 30-day washing schedule for the plant may not be adequate;
- matter deposition on heliostat surfaces is highly dependent on the location of the heliostat in the field; washing frequency may therefore also be a function of the location of the heliostat in the field.

In conclusion, the intra-plant air quality impacts may be the most important air quality concerns associated with a coal/solar hybrid plant of the size treated in this study.

8.2 Future Work

Additional air quality analysis needs to be done in at least a preliminary fashion before the evaluation of the air quality issues associated with a coal/solar hybrid plant can be considered completed. This section discusses unfinished tasks that are recommended for completion, most of which concern extra-plant impacts.

8.2.1 Crop Dusting

Because agriculture could exist close to the heliostat field, crop dusting could inadvertently result in the spraying of chemicals which are carried onto the surface of the heliostats, thereby adversely affecting heliostat performance. In order to estimate the impact of crop dusting on heliostat operation, the following tasks need to be accomplished:

- determine proximity of agricultural areas to the heliostat field;
- determine crop types near site;
- determine frequency of crop dusting in those areas;
- use a model to estimate pesticide coverage of the heliostat field (8.1);
- relate deposition of pesticide on a heliostat to degree of impairment of heliostat efficiency.

8.2.2 Effects of Solar Beam on Coal Plume

The issue of concern here is whether or not operation of the solar subsystem would exacerbate air quality problems associated with coal plants. Specifically, we are interested in determining whether secondary pollutants would form more rapidly if the plume from the coal stack crosses the solar beam than if no solar beam were present. Specific tasks for this problem include:

- determine under what conditions the plume from coal combustion could enter the solar beam;
- determine if sufficient time could elapse before the plume enters the beam so that significant amounts of nitric oxide can be converted to nitrogen dioxide (NO_2 is needed for the photochemical smog mechanism);
- determine the wavelengths of radiation needed for the photochemical smog mechanism;

- identify possible reactions that could be accelerated if the proper conditions are met;
- estimate the added concentrations of these products;
- determine the impacts of these products on the plant and on the environment.

8.2.3 Impacts of Plant on Surrounding Air Quality

Most of the air quality impact assessments discussed in this Volume have dealt with intra-plant impacts; i.e., the effect of one sub-system on another. A "traditional" air quality impact assessment should be done for the plant to show that its operation will not prevent attainment or maintenance of the national ambient air quality standards. The South Coast Air Quality Management District (SCAQMD) should be contacted regarding the specific technical tools (emission factors, models, etc.), that they recommend for use in such impact assessments. The SCAQMD has published a document entitled "Handbook for the Preparation of Environmental Impact Reports," which may prove to be of some value in performing the impact assessment (8.2).

8.3 References

8.1 Miller, C.O. "A Mathematical Model of Aerial Deposition of Pesticides from Aircraft." Environ. Sci. Technol., 14:824-831 (1980).

8.2 South Coast Air Quality Management District. "Handbook for the Preparation of Environmental Impact Reports." SCAQMD, El Monte, California, 1977.

APPENDIX A: DESCRIPTION OF AEROSOL HELIOSTAT IMPACTION MODEL

A.1 Plume Characteristics and Plant Design

One objective of this study has been to quantify in at least a preliminary way the deposition of particles on the surfaces of the heliostats. Thus the effects of the emissions of various substances on heliostat performance can be estimated. This section describes a crude mathematical model that was developed to quantify these deposition rates. Much of the section is oriented towards estimating the impacts of an elevated source; however, the basic principles of the model are applicable to both ground and elevated sources.

The coal combustion and salt particle emissions were assumed to be in the 0.1 μ diameter size range. Studies have shown that particles with diameters in the 0.1-1.0 μ range and densities of 1 gm/cm^3 will be diffused by turbulence in the same manner as gas molecules; particles in the 0.1-1.0 range will generally follow turbulent eddies (A.1). Consequently, the particles emitted by the proposed facility will likely behave as gas molecules in the atmosphere. Their behavior will not be significantly affected by gravitational forces, and they will therefore not fall out of the atmosphere onto the heliostat surfaces; however, the particles will impact on the heliostat surfaces through the action of wind blowing generally perpendicular to these surfaces. The heliostat array will thus act much like a series of baffles, removing particles which adhere and do not follow the air flow around the heliostat.

Computing the particle impaction rate can be done by multiplying the ambient particle concentration in $\mu g/m^3$ by the wind velocity in m/s. This will give a particle mass impaction rate on the cross-section represented by a heliostat in $\mu g/m^2$-sec. Given the height of the centerline of the plume and the average height of the heliostats, the downwind distance at which the plume will mix downward and begin to reach the heliostats can be estimated. According to the Gaussian model, the plume spreads vertically and horizontally with increasing distance from the source. We are interested at the distance at which the vertical spread (σ_z) becomes great enough to impact the heliostats.

The height of the heliostat can vary from 5 m, with the heliostat parallel to the ground, to 8.5 m, with the heliostat perpendicular to the ground. For the purposes of the modeling, we assume that the height of the heliostat is equal to twice the median height. The median height is 6.75 m, and twice that is nearly 20 m. The reason for this assumption is to allow for the uncertainty in the plume boundary. This is a worst-case assumption because it exposes more heliostats to the plume, and some are exposed to higher concentrations.

The height of the centerline of the plume was computed as 550 m; however, as a worst-case scenario, we assumed a plume rise of H = 440 m.

The plume expands downward as it moves downwind, as defined by the σ_z values. For example, with a centerline of 440 m and a (computed)

heliostat height of 20 m (the Rockwell plant), the plume will first start to impact the heliostats (with measurable particulate content) when $2\sigma_z$ = 440-20 = 420 m, or σ_z = 210 m. Twice σ_z is used as the criterion because most of the area under a Gaussian curve is within two standard deviations of the mean (plume centerline). Using plots of σ_z versus distance downwind (x) found in reference A.2, the distance downwind at which σ_z = 210 m under A stability (worst-case) is found to be approximately 700 m. When the downwind distance is 700 m, the horizontal dispersion coefficient (σ_y) is 155 m, so that $2\sigma_y$ = 310 m. The plume is therefore 620 m wide at that point.

Superimposing a map view of the plume on a map of the heliostat field will allow a determination of the total heliostat area exposed to a portion of the plume. For the Rockwell plant, all the heliostats from 700 m to the edge of the field (2400 m) were predicted to be affected by the plume.

Of particular interest, then, are the ambient concentrations of particulates at the exact location of each heliostat in the field. Multiplying this concentration by the wind speed immediately upwind of each heliostat will produce the mass impaction rate per unit cross-section area for that particular heliostat. Each heliostat will have a unique deposition rate because each heliostat is exposed to a different ambient concentration of particulates. This concentration is determined in part by two factors:

- plume behavior as predicted by the Gaussian model; concentration decreases with increasing distance from the source;
- depletion of the ambient concentration by the heliostat immediately upwind because some particles have adhered to the surface of the upwind heliostats.

The amount of particulate matter removed through impaction on a particular heliostat surface is further a function of:

- the angle of the heliostat, which is a function of its distance from the central tower; the angle influences the cross-sectional area exposed to the particle-carrying wind;
- the behavior of the particles in the air flow around and over the heliostat surface; this is a function of the size, shape and density of the particulates;
- the "sticking coefficient" of the particulate matter; a coefficient of 0 means that (averaged over a short time) none of the particulate matter carried through the cross-section cut out by the heliostat adheres, while a coefficient of 1 means that all of the particulate matter "permanently" adheres; in the absence of specific experimental data, a coefficient of 0.1 will be assumed in calculations.

Figure A-1 illustrates the various factors influencing the ambient particulate concentrations downwind of the stack.

Note that the model assumes, as a worst-case, that particulate matter that impacts the ground is not removed by the ground. Rather, this particulate matter is reentrained into the ambient air and is therefore "available" for impaction downwind on heliostat surfaces.

A.2 Phenomena Influencing Particle Impaction

The selection of a numerical value for the sticking coefficient should be made after considering the physical and chemical phenomena influencing particle impaction on solar collectors. Studies done by Sandia Laboratories at Albuquerque have found that electrostatic forces and very weak chemical bonding (Van der Waal's forces) are the primary mechanism by which natural particles (i.e., not these originating from coal combustion) adhere to solar collector surfaces. No evidence of chemical reactions between the adhered particles and the collector surfaces was observed. The adhesion process is thought to be grain-size dependent; a small grain size implies a large surface area, which in turn favors adhesion (A.3).

If particles from coal combustion behave in the same manner as natural soil particles, then the coal particulates should adhere strongly to the heliostat surface, because of their small size (0.1 to 1.0 μ diameter), provided the particles can once approach the surface at a close enough distance for the adhesion forces to take effect. One factor favoring the close passage of the particles over the heliostat surface is that the surface is likely to be cool, because the heliostats are efficient reflectors of radiant energy. Because of the absence of surface heating and turbulence over the heliostat surface, the microscale air flow over the surface is less likely to transport the particles away from the surface of the solar collector. A detailed study of the air flow around the heliostat surface accompanied by an extensive literature search on the forces influencing impaction of coal-combustion derived particulate matter on heliostat surfaces should be done in order to arrive at a reasonably accurate estimate of the probable magnitude of the sticking coefficient.

For the purposes of this study, we will assume that the sticking coefficient is 0.10. We are also assuming that the sticking coefficient does not vary with space or time. In reality, the coefficient will probably vary depending on wind speed and direction, temperature, humidity, degree of soiling of the heliostat surface, and other factors.

A.3 Model Description

The heliostat particulate impaction approach developed for this study is best used in a detailed computer analysis of plume behavior, particulate impaction, etc. Further refinements could be added to the model proposed, improving its accuracy. For the purposes of this paper, the model will be used in a simple way to derive admittedly crude estimates of the masses of particles deposited on the heliostat surfaces.

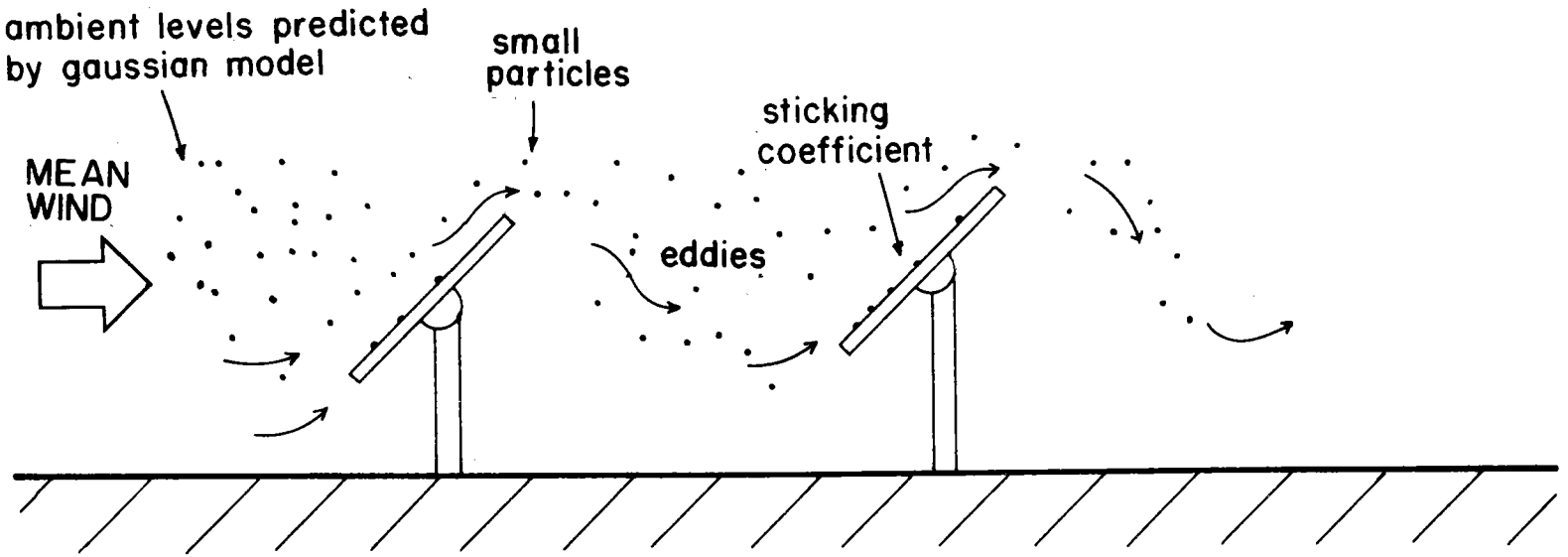

Figure A-1 Factors Influencing Particle Deposition Rates on Heliostats

We will assume that the following conditions exist:

- the wind does not change in speed or direction within the plant site;
- atmospheric stability does not change vertically or horizontally within the heliostat field;
- particulate concentrations reach a steady-state relative to re-entrainment from the ground;
- pollutants striking the ground are (mathematically) reflected upward;
- all heliostats are at the same angle (45°);
- particulates have a sticking coefficient of 0.1; that is, 10 percent of the particulates in the plume mathematically computed as passing "through" the cross-section of the heliostat come close enough to stick and by some mechanism do stick to the heliostat surface; 90 percent of the particles are passed on by.

From the standpoint of developing a worst-case scenario, a wind speed must be selected that will give a high impaction rate. For an elevated source the highest wind speed under A stability should be used. For a ground-level source, the highest wind speed under F stability that can occur at the site should be used.

For the purposes of this modeling exercise, individual heliostats will not be addressed; rather, the total heliostat area as given by the packing density of one cell will be used. The plume shape as predicted by the model is generally conical. However, for the purposes of this study fractions of heliostat cells were not addressed, and if a part of a cell was touched by the plume, then the whole cell was considered to be impacted. Resolution of 100 m in the Gaussian modeling is really not needed, because each heliostat cell is approximately 370 m on an edge; thus predicted ambient particulate concentrations only for about every 400 m are required as input by the model.

The predicted particulate deposition rates in kg per 300 day month were obtained with the following equation:

$$M = (c)(u)(S)(A)(N)(2.59 \times 10^{-3})$$

where

c = ambient particulate concentration predicted by the Gaussian model ($\mu g/m^3$)

u = mean wind speed in the 20 m boundary (m/s)

S = "sticking coefficient", the fraction of particles remaining on the heliostats after the Gaussian plume has (mathematically) impinged upon the heliostat surface

A = cross sectional area of the heliostat (m^2)

N = number of heliostats/cell

2.59×10^{-3} = constant to convert results to kg deposited per 30-day month

M = predicted mass (Kg) of particulates deposited per 30-day month

The cross sectional area of the heliostats was found by taking the sine of the angle of inclination and using it to compute the exposed height (h) of the heliostat in cross-section, as shown in Figure A-2.

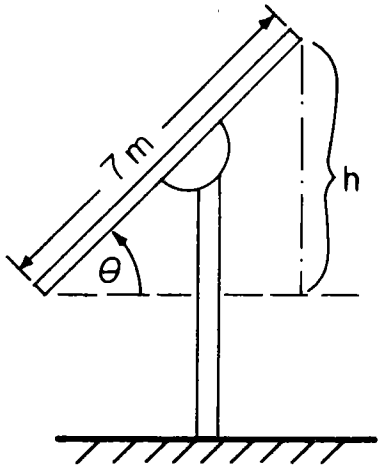

$\theta = 45°$ (in reality θ varies with time and space)

$\sin \theta \cong 0.7071$

$h = (0.7071)(7) = 4.9$ m

$A = (4.9 \text{ m})(7 \text{ m}) \cong 35 \text{ m}^2$

Figure A-2 Determination of Cross Section Area of Heliostat

Detailed use of the "sticking coefficient", S, would be as follows. At each heliostat location within the field the Gaussian plume computed as impacting that heliostat would lose a fraction, S, of its particulate content. The equation presented earlier in this appendix permits computation of mass deposition rates at each such point, and hence a "negative source" contribution to the plume made by the heliostats' "sticky" surface. Each heliostat thus contributes to a reduction in further downwind plume concentrations, which in turn can be computed through superposition can provide "corrected" downwind plume particulate content. A succession of such calculations, allowing appropriate parameter variations, would lead to detailed and potentially precise results.

However, the quantities actually removed from the plume by early deposition are small enough (several precent) to merit neglect in the present treatment. Other factors where we must use rough estimates are no doubt of greater importance. Thus we here assume deposition from a "virgin" plume impacting the entire field of heliostats.

A.4 Model Accuracy

The accuracy of the modeling exercise should be discussed so that the computed results can be placed in the proper context. Turner states that the major source of error in the Gaussian model is the vertical dispersion coefficient, which can be inaccurate anywhere from a factor of 5 to a factor of 10 for unstable conditions (A.4). The most accurate the Gaussian model can be is within a factor of three, including uncertainties in σ_z and the mean wind (A.5). This is in agreement with studies done by Fabrick, et al., who report that Gaussian models are accurate to within a factor of two to three for complex terrain (A.6). Turner summarizes the sources of errors in Gaussian models (A.7):

- characterizing the atmosphere with a single dispersion coefficient is an over-simplication;
- assuming complete eddy reflection at the ground and at the top of the mixing height is an oversimplification;
- there are errors in emission inventory information, source coordinates, physical source height and stack diameters, and variations in rate of fuel burned;
- wind speed at stack height is not the same as wind speed and direction at ground stations;
- input wind direction is not necessarily the direction of plume transport, because wind direction changes with height.

Additional uncertainty is introduced into model results because of the simplifying assumptions made in the heliostat impaction model. The model results should be interpreted to have an uncertainty of approximately a factor of five. Major sources of uncertainty in the heliostat impaction model include:

- uncertainties in the Gaussian plume model;
- all the plume particles may not be reflected from the ground;
- wind speed and direction are not the same for each heliostat;
- heliostat angles change with both time and distance, and are not fixed as assumed in the model;

- the "sticking coefficient" in reality may not be close to 0.10, as assumed in the model, due to chemical and physical phenomenon; further, it probably does not remain constant in time and space;

- the assumption that particle reentrainment reaches a steady-state equilibrium with ambient particle concentrations in the plume may not be valid.

Considering all the inaccuracies in the model results the data in Figures 3-8 and 3-9 should not be relied on in an absolute sense. Rather they should be interpreted as a possible concentration field to be expected under worst-case conditions.

A.5 References

A.1 Lewellen, W.S. and Y.P. Sheng. "Modeling of Dry Deposition of SO_2 and Sulfate Aerosols." Final Report Prepared for the Electric Power Research Institute by Aeronautical Research Associates of Princeton, Inc. Research Project Number 1306-1, EPRI Report Number EA-1452, July 1980, pages 4-1, 4-2, and Table 4-1.

A.2 Turner, A.B. "Workbook of Atmospheric Dispersion Estimates, U.S. Department of Health, Education and Welfare. PHSP No. 999-AP-26, 1969, p. 39.

A.3 Morris, V.L. "Cleaning Agents and Techniques for Concentrating Solar Collectors." Study done by Sandia Laboratories, Albuquerque Under Contract No. 13-0261, Printed by McDonnell Douglas Aeronautics Co., Huntington Beach, California, 1979.

A.4 Reference A.2, p. 7.

A.5 Reference A.2, p. 10

A.6 Fabrick, A., R. Sklarew and J. Wilson. "Point Source Model Evaluation and Development Study." Prepared by Science Applications, Inc., for the California Energy Resources Conservation and Development Commission under Contract Number A5-058-87, March 1977, p. 182.

A.7 Turner, D.B. "Atmospheric Dispersion Modeling, A Critical Review," J. Air Poll. Control Assoc., 29:502 (1979).